LETTER TO THE EDITOR

Dear Prof. Dr. Haynes,

this letter is to inform you about the revision of the ACPD manuscript (acp-2014-754) "Simulation of the isotopic composition of stratospheric water vapour – Part 2: Investigation of HDO/H_2O variations" by R. Eichinger, P. Jöckel and S. Lossow.

As requested by the referees and announced by our replies to their comments we have applied considerable revisions to the manuscript. This includes the incorporation of a new sensitivity study instead of the correlation analysis (which we decided was not sustainable). The abstract, introduction, discussion and conclusion sections have been adjusted accordingly. Thus, some parts of the discussion/conclusion (tropospheric/stratospheric influence on tape recorder, separation of large scale and convective clouds, underrepresentation of ice overshooting) are now (more) conclusively analysed, some other parts (separation of the two monsoon systems) are now only in the background of the study.

For your overview, here a summary of the main points:

1. We replotted all figures because of the new simulation we performed as part of the review process of the companion part 1 of the article. This also causes slight changes in the text, however, no changes in the conclusions.
2. We included a few sentences about the processes that influence δD(H_2O) in the model description section.
3. We added information about former evaluations of the model's hydrological cycle.
4. We added a general explanation for the dry bias in EMAC.
5. We merged the two tape recorder plots into a single figure.
6. We included an explanation for the enhancement of δD(H_2O) between 17 and 18 km being an artefact caused by seasonal averaging.
7. We restructured sections 5. and 6. and merged them into one section
   - The section now begins with an analysis of HDO and H_2O in the UTLS and the question, if it is in-mixing of old stratospheric air or tropospheric influences that causes the δD(H_2O) tape recorder.

- In Sect. 5.1, we now show that both effects contribute and that it likely is ice lofting that is important for the tropospheric part. For this, we added two figures for DJF corresponding to the JJA figures.
- The new sensitivity study is presented in Sect. 5.2. This supports our finding that tropospheric effects do have an influence on the δD(H_2O) tape recorder and secondly, also enables us to separate the effects of large-scale and from convective clouds.
- Finally, in Sect. 5.3, we conclusively describe the possible pathway of water vapour via the outflow of the monsoon systems into the stratosphere as an important contributor to the δD(H_2O) tape recorder.

8. The discussion and conclusion sections have been adapted accordingly. We still discuss the apparent stronger influence of the ASM compared to the NAM on the stratosphere in the model simulation and the discrepancy of this with ACE-FTS satellite data, however, suggest a more detailed analysis of this for a future study. Before that, however, more investigations on the underrepresentation of ice overshooting convection (which is now underpinned through the new sensitivity study) and its effect on the patterns are needed.
   Instead, we now conclude the separation of tropospheric and extratropical stratospheric influences on the δD(H_2O) tape recorder and moreover, distinguish between large-scale and convective clouds.

9. In the supplement, only minor changes have been conducted.

Please find below the differences between the discussion manuscript and the revised manuscript and the same for the supplement, as well as the comments of the referees and our corresponding answers.

Best regards
Roland, Patrick and Stefan

Simulation of the isotopic composition of stratospheric water vapour – Part 2: Investigation of HDO/H_2O variations

R. Eichinger[1], P. Jöckel[1], and S. Lossow[2]

[1]Deutsches Zentrum für Luft- und Raumfahrt e.V. (DLR), Institut für Physik der Atmosphäre, Münchner Straße 20, Oberpfaffenhofen, 82234 Weßling, Germany
[2]Karlsruhe Institute of Technology, Institute for Meteorology and Climate Research, Hermann-von-Helmholtz-Platz 1, 76344 Leopoldshafen, Germany

Studying the isotopic composition of water vapour in the lower stratosphere can reveal the driving mechanisms of changes in the stratospheric water vapour budget and therefore help to explain the trends and variations of stratospheric water vapour during the recent decades. We equipped a global chemistry climate model with a description of the water isotopologue HDO, comprising its physical and chemical fractionation effects throughout the hydrological cycle. We use this model to improve our understanding of the processes ~~,~~ which determine the patterns in the stratospheric water isotope composition and in the water vapour budget, itself. The link between the water vapour budget and its isotopic composition in the tropical stratosphere is presented through their correlation in a simulated 21 year time series. The two quantities depend on the same processes, however, are influenced with different strengths. A sensitivity experiment shows ~~,~~ that fractionation effects during the oxidation of methane ~~has~~ have a damping effect on the stratospheric tape recorder signal in the water isotope ratio. Moreover, the chemically produced high water isotope ratios overshadow the tape recorder in the upper stratosphere. Investigating the origin of the boreal summer ~~tape recorder signal in the lower stratosphere reveals~~ signal of isotopically enriched water vapour ~~crossing the tropopause over the subtropical Western Pacific. A correlation analysis confirms this link, which identifies the Asian Summer Monsoon as the major contributor for the intrusion of isotopically enriched~~ reveals that in-mixing of old stratospheric air from the extratropics and the intrusion of tropospheric water vapour into the ~~stratosphere during boreal summer. Moreover, convective ice lofting~~ stratsphere complement each other in order to create the stratospheric δD(H_2O) tape recorder signal. For this, the effect of ice lofting in monsoon systems is shown to ~~have a substantial impact on the isotope ratios of water vapour in the upper troposphere and lower~~ play a crucial role. Moreover, we describe a possible pathway of isotopically enriched water vapour through the tropopause into the tropical stratosphere.

Manuscript prepared for Atmos. Chem. Phys.
with version 5.0 of the LaTeX class copernicus.cls.
Date: 24 April 2015

Simulation of the isotopic composition of stratospheric water vapour – Part 2: Investigation of HDO/H_2O variations

R. Eichinger[1], **P. Jöckel**[1], **and S. Lossow**[2]

[1]Deutsches Zentrum für Luft- und Raumfahrt e.V. (DLR), Institut für Physik der Atmosphäre, Münchner Straße 20, Oberpfaffenhofen, 82234 Weßling, Germany
[2]Karlsruhe Institute of Technology, Institute for Meteorology and Climate Research, Hermann-von Helmholtz-Platz 1, 76344 Leopoldshafen, Germany

Correspondence to: R. Eichinger
(Roland.Eichinger@dlr.de)

Abstract. Studying the isotopic composition of water vapour in the lower stratosphere can reveal the driving mechanisms of changes in the stratospheric water vapour budget and therefore help to explain the trends and variations of stratospheric water vapour during the recent decades. We equipped a global chemistry climate model with a description of the water isotopologue HDO, comprising its physical and chemical fractionation effects throughout the hydrological cycle. We use this model to improve our understanding of the processes which determine the patterns in the stratospheric water isotope composition and in the water vapour budget, itself. The link between the water vapour budget and its isotopic composition in the tropical stratosphere is presented through their correlation in a simulated 21 year time series. The two quantities depend on the same processes, however, are influenced with different strengths. A sensitivity experiment shows that fractionation effects during the oxidation of methane have a damping effect on the stratospheric tape recorder signal in the water isotope ratio. Moreover, the chemically produced high water isotope ratios overshadow the tape recorder in the upper stratosphere. Investigating the origin of the boreal summer signal of isotopically enriched water vapour reveals that in-mixing of old stratospheric air from the extratropics and the intrusion of tropospheric water vapour into the stratsphere complement each other in order to create the stratospheric δD(H_2O) tape recorder signal. For this, the effect of ice lofting in monsoon systems is shown to play a crucial role. Moreover, we describe a possible pathway of isotopically enriched water vapour through the tropopause into the tropical stratosphere.

1 Introduction

Variations of stratospheric water vapour alter the radiative heat budget (Forster and Shine, 1999) and the ozone mixing ratios (Shindell, 2001). The processes which control the stratospheric water vapour budget, however, are poorly quantified (Fueglistaler et al., 2009). These processes are temperature-controlled dehydration, convective activity methane oxidation and isentropic transport.

Due to their physical and chemical properties, water isotopologues have the potential to answer the open questions concerning the origin of stratospheric water vapour. The small mass difference between H_2O and HDO ~~lead~~ (^{16}O, respectively; the hydrogen isotope deuterium D denotes ^2H) leads to different vapour pressures and zero-point energies. This causes equilibrium and kinetic fractionation effects during phase changes and chemical reactions. Each process ~~,~~ which controls the stratospheric water vapour budget can be associated with certain fractionation effects and therefore ~~,~~ leaves a specific isotopic signature in the water vapour compound (see Moyer et al., 1996; Steinwagner et al., 2010). This isotopic fingerprint allows to comprehend the history of stratospheric water vapour (Johnson et al., 2001) and therewith, can assist to explain the trends and variations of its budget.

In addition to in situ and remote sensing measurements, the comprehensive simulation of the physical and chemical processes of water isotopologues on the global scale is needed to gain an improved understanding of the basic structure of the water isotope ratios in the stratosphere. Model studies of water isotopologues in the upper troposphere lower stratosphere (UTLS) include approaches from conceptional

(Dessler and Sherwood, 2003; Bolot et al., 2013), to one-dimensional (Ridal et al., 2001; Zahn et al., 2006) and two-dimensional (Ridal and Siskind, 2002) models. Schmidt et al. (2005) applied the general circulation model (GCM) GISS-E, in order to study stratospheric entry values of the isotope ratios of water vapour. However, this model has a comparatively low resolution in the stratosphere and the accounting for methane oxidation is prescribed with a fixed production rate.

In the companion part 1 of the article (Eichinger et al., 2014) an extension of the global climate chemistry model (CCM) EMAC (ECHAM MESSy Atmospheric Chemistry) was presented and evaluated. This extension, namely the H2OISO submodel, comprises ~~a separate~~ an additional hydrological cycle, including the water isotopologues $H_2^{18}O$ and HDO and their physical fractionation effects, based on previous studies by e.g. Hoffmann et al. (1998) and Werner et al. (2011). Besides ~~using sufficient vertical resolution that~~ a vertical resolution resolving the tropical tropopause layer (TTL) ~~is well resolved and explicit stratospheric dynamics~~ and simulating the stratospheric dynamics explicitely, this expanded model system also includes the computation of the methane isotopologue CH_3D and its chemical contribution to HDO through oxidation. Results of an EMAC simulation showed good agreement in stratospheric HDO and δD(H_2O) ~~($\delta D(H_2O) = \frac{[HDO]/[H_2O]}{R_{VSMOW}}$; ($R_{VSMOW} = 155.76 \cdot 10^{-6}$; Hagemann et al., 1970); VSMOW: Vienna Standard Mean Ocean Water)~~

$$\delta D(H_2O) = \left(\frac{[HDO]/[H_2O]}{R_{VSMOW}} - 1 \right) \cdot 1000 \quad (1)$$

with measurements from several satellite instruments. ~~Moreover, they~~ The Vienna Standard Mean Ocean Water VSMOW (IAEA, 2009) HDO standard is $R_{VSMOW} = 155.76 \cdot 10^{-6}$, (see Hagemann et al., 1970). Moreover, the results revealed a stratospheric tape recorder ~~,~~ which ranges between the pronounced signal of MIPAS observations (see Steinwagner et al., 2010) and the missing upward propagation of the seasonal signal in the ACE-FTS retrieval (see Randel et al., 2012).

The results of ~~this simulation~~ these simulations are now further analysed, aiming to identify the processes ~~,~~ which determine the patterns of the isotopic signatures in stratospheric water vapour. The connection between the water vapour budget and its isotope ratio in the tropical stratosphere over the two simulated decades is presented in Sect. 3. The influence of isotope effects during methane oxidation on the δD(H_2O) tape recorder signal is investigated in Sect. 4. In Sect. 5 ~~and Sect. 5.1 the~~ the origin of the Northern Hemisphere (NH) summer signal of the δD(H_2O) tape recorder is ~~traced back to its origin, by examining the contributions of different Monsoon Systems and convective ice lofting on the isotopic compsition of water vapour in the UTLS.~~ examined. Its exclusive generation in the NH is shown to be connected with in-mixing of extratropical air and ice lofting in association with clouds in monsoon systems. Furthermore, a possible pathway of isotopically enriched water vapour from the NH troposphere into the tropical stratosphere is presented. These analyses also reveal a possible underestimation of ice overshooting in the applied convection scheme ~~,~~ which can have a significant effect on δD(H_2O) in the lower stratosphere. This study constitutes the ~~initiation of the~~ first application of the ~~new process diagnostics provided by the~~ isotopic composition of water vapour ~~for exploring~~ in order to explore the reasons for changes in the stratospheric water vapour budget ~~in~~ with global atmosphere chemistry-climate models.

2 Model description and simulation setup

The ~~MESSy-conform H2OISO submodel~~ MESSy submodel H2OISO in the framework of the EMAC model (Jöckel et al., 2005, 2010) comprises ~~a separate~~ an additional (and separate from the actual) hydrological cycle, including tracers (Jöckel et al., 2008) for the water isotopologues $H_2^{16}O$, HDO and $H_2^{18}O$, in the three phases (vapour, liquid and ice), respectively. These tracers are treated identically to the standard state variables for water in the regular hydrological cycle of EMAC, with the addition of the physical fractionation effects for the isotopologues during phase transitions. The representation of these effects follows the water isotopologue-enabled ECHAM (ECMWF Hamburg) model ~~versions (see Hoffmann et al., 1998; Werner et al., 2001, 2011).~~ (see Hoffmann et al., 1998; Werner et al., 2001, 2011). Equilibrium and kinetic fractionation during the evaporation of water from oceans is described by the bulk formula of Hoffmann et al. (1998). Due to the limitations of the applied land surface scheme we neglect any isotope fractionation from land surfaces (for details, see Werner et al., 2011). The implementation of the cloud and convection parameterisations (CLOUD and CONVECT) in EMAC follows the study of Werner et al. (2011). For condensation within clouds and for the evaporation of cloud water, a closed system is assumed. An open system is used for the deposition of water vapour to ice. Due to the low diffusivities of the isotopologues in the ice phase, no exchange happens between ice and vapour. During the melting of ice and the freezing of water, as well as for the sedimentation of ice, autoconversion, accretion and aggregation, no fractionation is assumed. The representation of the fractionation during reevaporation of raindrops follows the study by Hoffmann et al. (1998) who assume an isotopical equilibration of 45% for large drops from convective rain and 95% for small drops falling from stratiform clouds. Supplementary, an explicit accounting for the contribution of CH_3D oxidation to HDO, including a parameterisation of the deuterium storage in molecular hydrogen, has been developed ~~,~~ in order to achieve realistic HDO mixing ratios and δD(H_2O) values in the stratosphere.

In the companion part 1 of this article (Eichinger et al., 2014), the model system and the implementation of HDO throughout the hydrological cycle, including its chemical representation~~is~~ , are presented in detail.

An EMAC simulation in the T42L90MA (∼2.8°×2.8°, 90 ~~vertical layers~~ layers in the vertical - up to 80 km (0.01 hPa), explicit middle atmospheric dynamics) resolution was carried out. The simulation was performed with specified dynamics (i.e., "nudged" towards ERA-Interim reanalysis data (ECMWF; Dee et al., 2011) up to 1 hPa). The "Tiedtke-Nordeng" convection scheme (Tiedtke, 1989; Nordeng, 1994) was applied for the simulation. After starting from steady-state initial conditions in 1982, the simulation was evaluated during the 21 years from 1990 to ~~2011.~~ the end of 2010. A detailed description of the simulation setup ~~,~~ and a description of the applied MESSy submodels ~~and an~~ are presented in the companion part 1 of this article (Eichinger et al., 2014) . An evaluation of the model's hydrological cycle itself can be found in Hagemann et al. (2006) who assess the EMAC basemodel ECHAM5. Jöckel et al. (2006) state that the modifications introduced by the MESSy system, as well as by the application of the T42L90MA resolution and nudging, produces a hydrological cycle similar to the results by Hagemann et al. (2006) and consistent with observations. An extensive evaluation of the ~~simulation is given in~~ isotopic composition of water vapour and of its chemical precursor CH_3D in this EMAC simulation in the troposphere and the stratosphere is presented in the companion part 1 of ~~this~~ the article (Eichinger et al., 2014). Overall, a reasonable representation of stratospheric HDO is concluded, however, with some systematic, but explainable, discrepancies.

3 Time series of H_2O and $\delta D(H_2O)$

Temporal variations in stratospheric water vapour during the last decades have been observed ~~consistently~~ by various instruments. The reasons for these variations are much discussed ~~(see e.g. Hurst et al., 2011; Dessler et al., 2013; Randel and Jensen, 2013)~~. Before analysing these changes with the EMAC model using the newly implemented HDO, it has to be assured that the EMAC simulation features the main characteristics of the changes in stratospheric water vapour from 1990 to ~~2011.~~ the end of 2010. Therefore, the equatorial water vapour mixing ratios at 30 km altitude of the simulation are compared with a combined HALOE (HALogen Occultation Experiment) and MIPAS data set in Fig. 1. A detailed description of the combination of the satellite data time series is given in the supplement. A two year running mean was calculated for both time series in order to make the trends more visible by eliminating the signal of the quasi-biennial oscillation (QBO).

The combined HALOE/MIPAS ~~observations~~ data show an increase in stratospheric water vapour in the first half of the 1990s and a plateau hereafter until the year 2000. The water vapour mixing ratio drops by around 0.3 μmol/mol between 2000 and 2002 and stays at this lower level until the middle of the first decade of the 21st century. Hereafter, a slow increase can be observed until the end of the time series in ~~2012.~~ 2010. This behaviour of stratospheric water vapour during the previous decades has also been reported and discussed e.g., by Randel and Jensen (2013) analysing a combined HALOE and MLS (Microwave Limb Sounder) data set, and is strongly connected to tropopause temperatures.

The EMAC simulation generally reproduces these variations, although with a constant offset and a few differences. The general dry bias in EMAC has already been discussed by Jöckel et al. (2006) and in the companion part 1 of the article (Eichinger et al., 2014) . Its main reasons are the slightly too cold hygropause in the nudging data (see e.g., Liu et al., 2010) and the coarse horizontal resolution of the model. In contrast to the satellite observations, in the EMAC simulation the drop around the year 2001 is preceded by an increase in water vapour. ~~Moreover, in contrast to the satellite observations, the~~ Moreover, the level of the water vapour mixing ratio after the drop does not fall below the level of the early 1990s. The Pearson's correlation coefficient between the observed and simulated time series is $R^2 = 0.50$.

In order to estimate the correlation between the changes of water vapour and its isotopic composition, the monthly anomalies w.r.t. the 21 year monthly averages of the tropical water vapour mixing ~~ratio~~ ratios and $\delta D(H_2O)$ are shown in Fig. 2 for the 21 years of the EMAC simulation at 18 km and at 30 km altitude, respectively. Again, the data was processed with a two year running mean, in order to obtain a better visibility of the trends. The anomaly of $\delta D(H_2O)$ is scaled with $1/30$ for better comparability.

At 18 km altitude, the Pearson's correlation ~~(a description is given in the supplement)~~ coefficient between the two time series is ~~0.58~~ $R^2 = 0.57$ and this correlation decreases to ~~0.27~~ $R^2 = 0.28$ at 30 km. At 18 km altitude, ~~the~~ both quantities are dominated by tropospheric and change processes~~are determining for both quantities~~. At 30 km altitude, the chemical effects, induced by CH_4 oxidation for H_2O and the different life times of CH_4 and CH_3D for $\delta D(H_2O)$ ~~, are dominating~~become important. An interdependence of the two quantities can be observed at both altitudes, although, during certain periods, the development of the two time series is ~~opposing~~anticorrelated. The drop around the year 2001 can be seen in water vapour and in $\delta D(H_2O)$ at both altitudes. At 18 km, the more pronounced feature in $\delta D(H_2O)$, however, is the steep increase before the drop. The amplitude of this increase in $\delta D(H_2O)$ exceeds the amplitude of the drop almost by a factor of 2. Even though most of the variations of the two quantities are

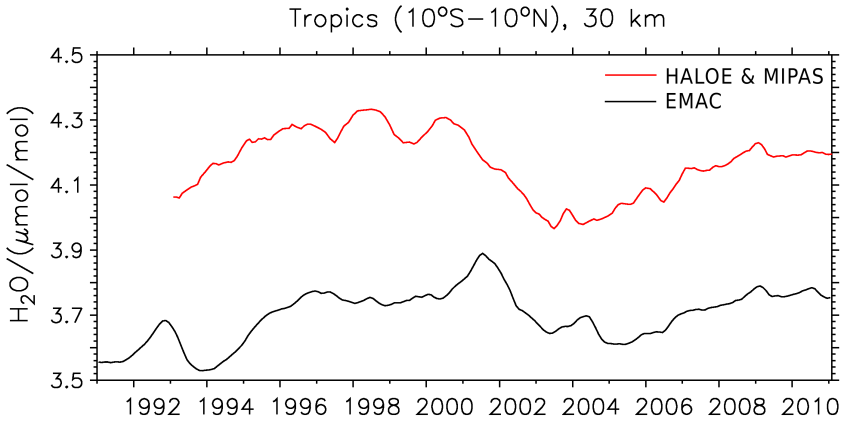

Fig. 1. Time series of stratospheric ~~(at)~~ water vapour at 30 km averaged between 10°S and 10°N. Combined HALOE and MIPAS data and the EMAC simulation. Both time series are processed with a two year running mean.

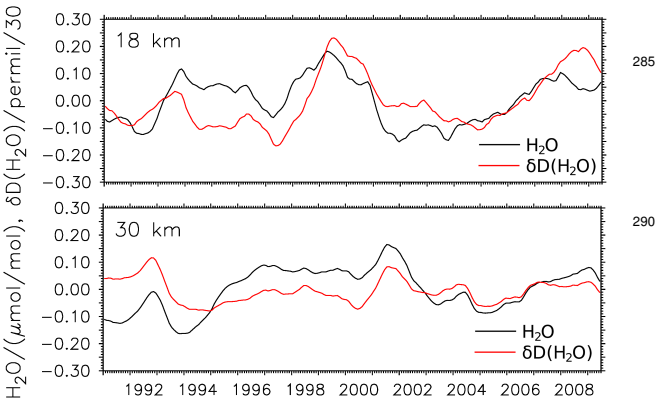

Fig. 2. Time series of EMAC simulated monthly stratospheric water vapour (black) and δD(H_2O) (red) anomalies w.r.t. the 21 year monthly average at 18 km and at 30 km altitude, averaged between ~~10~~15°S and ~~10~~15°N and processed with a two year running mean filter. The δD(H_2O) anomalies were scaled with the factor 1/30 for better comparability.

~~oriented similarly, the sign~~ in phase, the signs of the anomalies ~~is sometimes opposing~~are sometimes inverted. At 18 km altitude, δD(H_2O) is generally at a lower level at the end of the 1990s compared to the early 2000s, after the drop. The short-term changes in particular seem to be different between the two quantities. This suggests, that the processes that control stratospheric δD(H_2O) are related, but not equal to those that control the stratospheric water vapour budget. The tropopause temperatures, methane oxidation, convective activity or other processes determining water vapour in the stratosphere are thus affecting stratospheric H_2O and δD(H_2O) with different strengths. Knowledge of this behaviour can therefore help to address the origin of certain variations and trends to changes in specific processes. The next sections are thus aiming on ~~working out~~ revealing the influence of individual processes on stratospheric δD(H_2O), with a special focus on the tape recorder, since the strength of this phenomenon largely determines the intrusion of water vapour into the stratosphere.

4 Sensitivity of the δD(H_2O) tape recorder to methane oxidation

In order to analyse the impact of the contribution of CH_4 and CH_3D oxidation on the δD(H_2O) tape recorder signal, an additional EMAC simulation was conducted. The only difference of this simulation is a modified chemical tendency for HDO. The concept for this sensitivity simulation is an artificial deactivation of the chemical fractionation effects. In other words, δD(H_2O) does not get influenced by chemical isotope effects, CH_3D oxidation alters HDO always in relation to CH_4 oxidation, as if there was no isotope fractionation. A detailed description of this modification is given in the supplement.

For the analysis of the impact of isotope effects during methane oxidation on the δD(H_2O) tape recorder signal, the simulation with modified HDO tendency is compared to the simulation with regular methane isotope chemistry. The setup is the same for both simulations. ~~Figs~~Fig. 3 ~~and ?? show~~ shows the tropical tape recorder ~~signal~~ signals from 2004 to 2009 for the two simulations from 15 to 30 km.

~~Tropical (15°S-15°N) δD(H_2O) tape recorder signal from 2004 to 2009 in the simulation without the effect of methane oxidation on δD(H_2O).~~

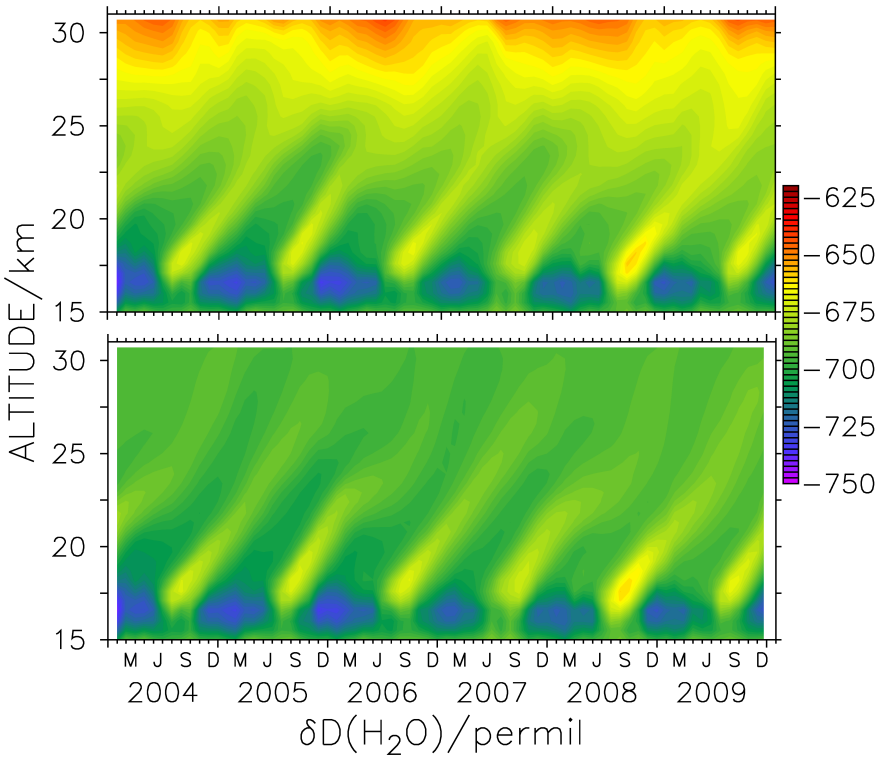

Fig. 3. Tropical (15°S-15°N) δD(H_2O) tape recorder signal from 2004 to 2009 in the simulation including (upper panel) and without (lower panel) the effect of methane oxidation on δD(H_2O).

Between 15 and 25 km the δD(H_2O) values are similar in both figures. In the tropical tropopause layer and the lower stratosphere, δD(H_2O) is only weakly affected by methane oxidation. From 25 km upwards, increasingly higher δD(H_2O) values can be observed in ~~Fig. 3.~~ the simulation with regular methane isotope chemistry (upper panel). The effect of the chemistry on δD(H_2O) increases with altitude in the stratosphere. This can be observed for the increased δD(H_2O) values, which emerge during NH summer, as well as for the low δD(H_2O) values from the boreal winter signal. The tape recorder signal in ~~Fig. ?? is stronger and~~ the simulation with modified methane isotope chemistry (lower panel) reaches higher up. It is still present, although weak, at the top of the figure at around 30 km altitude. In ~~Fig. 3 the~~ the upper panel the δD(H_2O) tape recorder signal above 25 km ~~is entirely~~ becomes increasingly overshadowed by high δD(H_2O) values, which are generated by the different life times of CH_4 and CH_3D~~.~~, i.e. chemical isotope effects. The upward propagating signatures fade out, or rather mix ~~in~~ with the high δD(H_2O) values. These high δD(H_2O) values show variations with a phase of around two years which can be associated with the QBO.

For a better quantification of the differences of the two tape recorder signals, Fig. 4 shows the ~~averaged amplitudes~~ annually averaged difference of the δD(H_2O) ~~tape recorder signals with altitude .~~ maximum and minimum as function of altitude for the time period of Fig. 3. The black line denotes the simulation with, and the red line the simulation without the methane effect.

The tape recorder amplitudes are equal below ~~the lower stratosphere~~20 km. As expected, further above, the amplitude of the simulation with chemistry effect on δD(H_2O) decreases faster with altitude than the amplitude of the simulation without this effect. The high δD(H_2O) values from the NH summer signal are not affected as strongly by methane oxidation as the low values from the NH winter signal. To explain this, constant temperatures, and hence fractionation factors, and a constant background δD(CH_4) are assumed, which is reasonable here. The isotope ratios of isotopically different reservoirs ~~possess~~ show different sensitivities to the addition of a compound with a certain isotope ratio. This means that the smaller the differences between the δ values are, the smaller is the ~~alteration~~modification. Since the high δD(H_2O) values from the NH summer signal are closer to the δD(CH_4) values (δD(CH_4) is also based on VSMOW)~~values~~, which are around $-50‰$ here, compared to the low δD(H_2O)

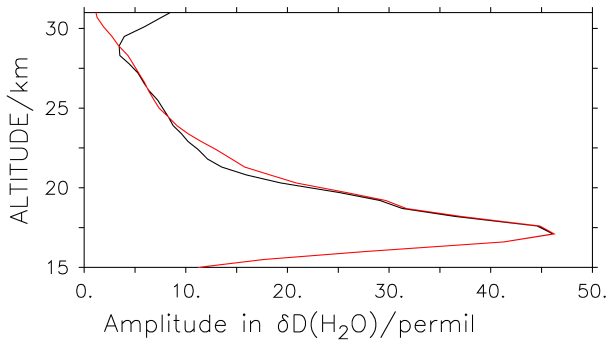

Fig. 4. ~~Averaged annual amplitudes~~ Annually averaged difference between the maximum and the minimum of δD(H_2O) ~~with~~ as function of altitude, with (black) and without (red) the effect of methane oxidation on δD(H_2O).

values from NH winter, the summer signal is altered less. Additionally, also the water vapour mixing ratios are different here. The δD(H_2O) values of the low water vapour mixing ratios from the NH winter signal are therefore again affected ~~stronger~~ more strongly by the addition of (a similar amount of) isotopically enriched water vapour from methane oxidation. This concludes that the production of H_2O and HDO by the oxidation of CH_4 and CH_3D, reduces the amplitude of the δD(H_2O) tape recorder and overshadows the upward propagation of the signal.

~~Above~~ Between 24 and 28 km, the amplitude of the δD(H_2O) variations ~~of~~ in the simulation with chemistry effect on δD(H_2O) are similar and above 28 km the amplitude in the simulation with the chemistry effect exceeds the amplitude of the simulation without. This, however, is not due to the tape recorder effect anymore~~. It is due to temperature and hence chemical fractionation factor variations~~ , but caused by the QBO. The QBO also has an effect on the stratospheric water vapour budget and on the water vapour tape recorder (see Niwano et al., 2003) . As stated above, the cycle of the QBO can be seen in the high δD(H_2O) values between 25 and 30 km in Fig. 3. ~~The QBO also has an effect on the stratospheric water vapour budget and on the water vapour tape recorder (see Niwano et al., 2003)~~ Temperature and hence chemical fractionation factor variations and also dynamical differences between the QBO phases which mix-in more or less strongly enriched water vapour lead to this cycle and hence to this increase in amplitude.

5 The origin of the δD(H_2O) tape recorder

5.1 ~~The pathway of isotopically enriched water vapour into the tropical stratosphere~~

~~In order to analyse the origin of the~~ Both, the water vapour mixing ratio and δD(H_2O)~~tape recorder signal, the zonal and seasonal means, averaged over the 21 years of the EMAC simulation~~ , exhibit enhanced values in the lower stratosphere during JJA (June, July, August)~~between 10 and are presented in Fig. ??. In~~ . The underlying processes for this, however, may differ in some ways for the two quantities. In order to demonstrate this and to analyse the origin of the tape recorder signal, the ~~supplement, this illustration is also presented for the other seasons (DJF - December, January, February; SON - September, October, November; MAM - March, April, May) .~~ water vapour mixing ratios and δD(H_2O) in the UTLS for JJA are shown in Fig. 5.

~~High δD(~~Differences in the distribution of the enhanced values can be observed when comparing the two panels. In the left panel, enhanced H_2O ~~) values~~ mixing ratios can be seen ~~in the troposphere and in the high latitudesof the upper stratosphere. The minimum in~~ within almost the entire TTL, however, decreasing with altitude and towards the southern latitudes. At the northern edge of the TTL, the high H_2O mixing ratios exceed the tropopause and penetrate into the stratosphere. Some water vapour, however, also intrudes into the stratosphere in the central and the southern TTL. Isotopically enriched water vapour (see right panel) exclusively enters the stratosphere at the northern edge of the TTL. δD(H_2O) ~~can be found around the tropical tropopause . This minimum spreads out to the poles at around and to the upper tropical stratosphere. In the Northern Hemisphere an elevated signal of high tropospheric isotope ratios can be observed around 40°N. At the~~ values of above $-650‰$ can be observed, crossing the tropopause and entering the tropical pipe here. Note that the enhancement of δD(H_2O) between 17 and 18 km is an artefact caused by the seasonal averaging. The signal originates from the northern edge of the ~~tropical tropopause layer, this isotopically enriched water vapour penetrates into the stratosphere along the isentropes, through the tropopause, into the tropical pipe~~ TTL and remains in the tropical pipe during summer while being mixed with surrounding air masses comparatively quickly between 16 and 17 km. In the ~~tropics the maximum of this signal is transported upwards across the isentropes. It can still be seen during SON , but hardly during DJF (see supplement) . An elevation of enhanced~~ supplement, zonal δD(H_2O) across all latitudes is also presented for the other seasons (DJF - December, January, February; SON - September, October, November; MAM - March, April, May) from 10 to 30 km altitude. There, the high δD(H_2O) values ~~during JJA can also be seen in the northern extratropics up to . These, however, mix in with the depleted stratospheric~~ in the tropical pipe can still be seen during SON and DJF. In the central and southern parts of the TTL, the water vapour is isotopically strongly depleted, exhibiting values below $-700‰$. Low δD(H_2O) values ~~much quicker than in the tropics and are already not visible anymore in SON~~can be observed down to 14 km altitude in the central and southern TTL, while

~~Zonally and seasonally averaged $\delta D(H_2O)$ (coloured), tropopause height (black line) and isentropes (blue contour lines) in K for JJA, averaged over the 21 years of the EMAC simulation.~~

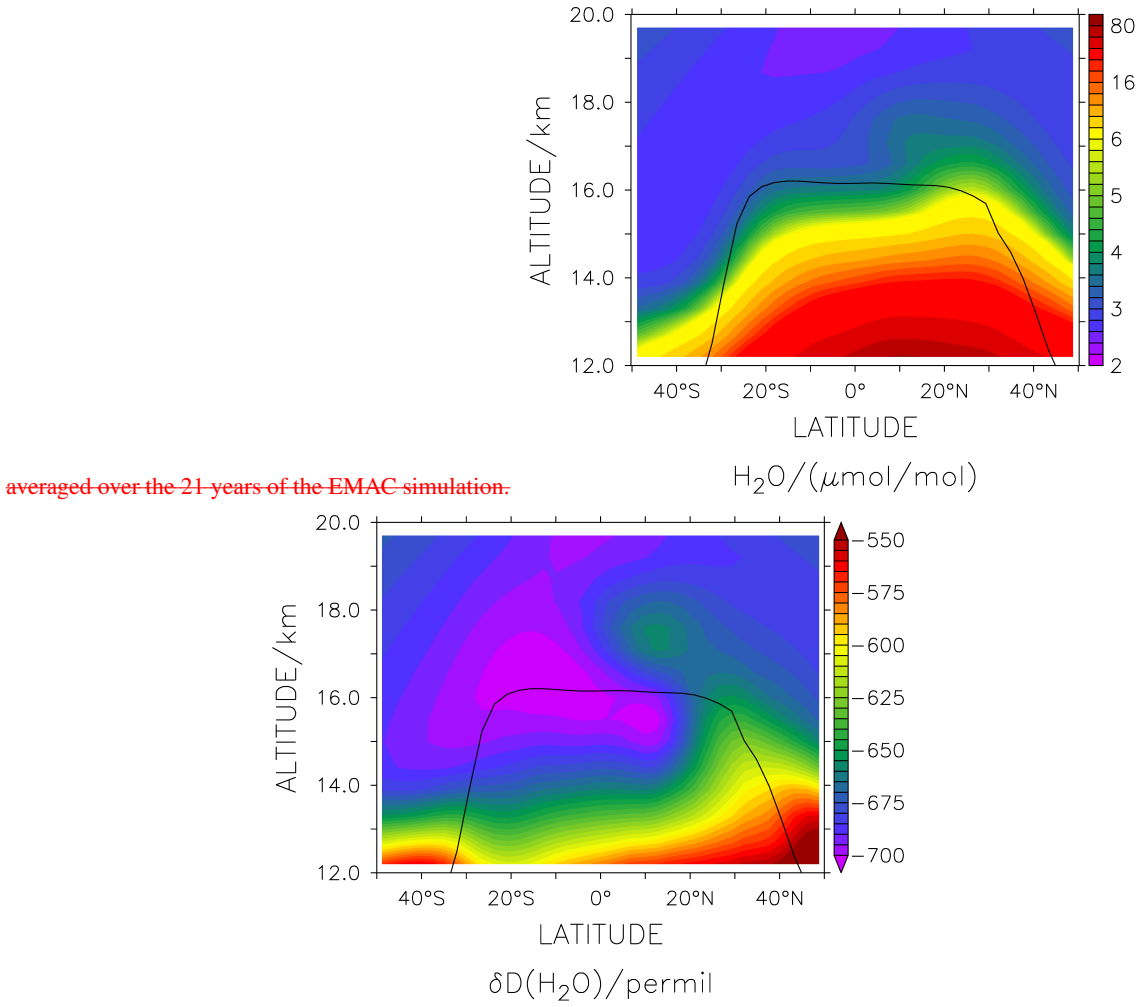

Fig. 5. H_2O mixing ratio (left panel) and $\delta D(H_2O)$ (right panel) in the UTLS in JJA averaged over the 21 years of the EMAC simulation. The black lines denote the tropopause.

relatively high water vapour mixing ratios reach up to almost 16 km altitude in this region.

In this illustration, in contrast to H_2O, the origin of the enhanced isotope ratios in the tropical lower stratosphere during JJA, can ~~clearly be associated with elevated isotopically enriched water vapour in the northern hemispheric troposphere. A similar elevation~~ be seen exclusively in the NH. However, it is not clear if it originates from the intrusion of tropospheric water vapour into the stratosphere or from in-mixing of old stratospheric air from the extratropics. During DJF a similar signal of isotopically enriched ~~tropospheric water vapour can also be observed during DJF at~~ water vapour at the edge of the TTL at around 40°S can be observed (see supplement). In contrast ~~,~~to JJA, here this signal is at considerably lower altitudes and does not penetrate into the ~~tropical~~ stratosphere.

~~When entering~~ In the lower stratosphere, air experiences rapid horizontal transport between the tropics and the mid-latitudes above the subtropical jets (Rosenlof et al., 1997). The region between the 380 and the 400 K isentrope is therefore crucial for the properties of stratospheric air. To provide an insight into the horizontal dynamics of this region, the average of $\delta D(H_2O)$ between the 380 and the 400 K isentrope is shown in a latitude-longitude representation ~~during~~ for JJA in Fig. 6. Again the other seasons are presented in the supplement.

In general, the image features a pattern with low $\delta D(H_2O)$ in the tropics and increasing values with higher latitudes. In the Northern Hemisphere, patterns can be observed ~~,~~which are associated with the Asian Summer Monsoon (ASM) ~~, as~~

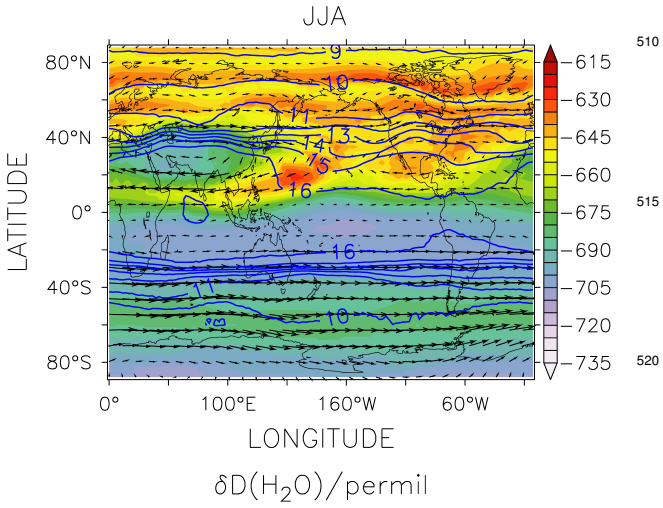

Fig. 6. Seasonally averaged δD(H_2O) (colours), horizontal wind vectors (arrows) averaged from the 380 to the 400 K isentrope and the tropopause height in km (blue contour lines) in JJA, averaged over the 21 years of the EMAC simulation.

~~well as with~~ and the North American Monsoon (NAM). High δD(H_2O) values can be seen over the entire North American continent. Over southern Asia, in contrast, very low values are dominant. Around this isotopically depleted centre of the ASM anticyclone, the water vapour is isotopically enriched. Over the Western Pacific, ~~the~~ at the outflow of the ASM anticyclone, the wind vectors indicate a considerable southward component, which drags isotopically enriched air from the extratropics towards the tropics and westwards hereafter. This air ~~originates from the westerly wind regime at around 40°N over the Asian continent, because a high potential vorticity gradient (not shown) north of this region prevents meridional air mass exchange (see e.g. Plumb, 2002) . In the Western Pacific region, furthermore, a lowering of the tropopause is evident. This is likely to be the region where water vapour can enter the stratosphere.~~

~~In order to identify the origin of the high δD(H_2O) values over the Western Pacific, a zonal cross section, averaged from 30°N to 40°N is presented in Fig. 11.~~

~~Zonal cross section of δD(H_2O), averaged from 30°N to 40°N for JJA (averaged over the 21 years of the EMAC simulation). The black line denotes the tropopause height, the red contour lines indicate levels of constant potential temperatures (isentropes).~~

~~Here, the highest tropospheric δD(H_2O) values can be found at around 100°E, above the Himalaya mountains. Another, yet weaker, maximum lies at around 100°W, which is the location of the Mexican High Plateau and the NAM. A third, even weaker maximum at 0°E can be associated with the North African Monsoon. The lowest values are accompanied by the highest parts of the tropopause, which lies at around altitude at 50°E. This is also where the temperatures are lowest (not shown). The tropopause height exhibits two minima, one around 160°W and one around 10°W. In these minima, the highest stratospheric δD(H_2O) values are found. The underlying westerly wind regime (shown in Fig. 6), connected with the tropopause-crossing isentropes in the subtropics, is thus confirming that the enhanced stratospheric isotope ratios during JJA originate from monsoonal (Asian and American) activity. Isentrope-crossing upward motion of the isotopically enriched water vapour in this region can be explained with strong gravity wave activity, taking place within the jetstreak at the forefront of the ASM anticyclone (see e.g., Reid and Gage, 1996) .~~

~~These high δD(H_2O) values are much more pronounced for the ASM and referring to Fig. 6, only the Western Pacific region provides a strong enough southward wind component to transport this isotopically enriched water vapour into the tropics. This suggests, that the NH summer signal of the stratospheric δD(H_2O) tape recorder, which propagates upwards over time, is mainly generated by the ASM.~~

~~In order to confirm this assumption, Fig. **??** shows the difference in δD(H_2O) between the two main Monsoon regions (a subtraction of the average of 140°W to 40°W from the average of 80°E to 180°E); in other words, the ASM region minus the NAM region. For guidance, the tropopause and the isentropes (averaged globally) are included here as well. Positive values indicate higher δD(H_2O) in the Western Pacific, negative values show enhanced δD(H_2O) in the American region.~~

~~Difference in δD(H_2O) between the zonal average from 80°E to 180°E and from 140°W to 40°W for JJA (ASM minus NAM). The thick line shows the zonally averaged tropopause and the thin contour lines denote the isentropes (both globally averaged).~~

~~The most dominant feature of the figure is the patch of very high values in the northern TTL, between 12 and . This indicates that in the model, convective activity is much stronger in the Western Pacific region than in the American region. Another region with high values can be found above the tropical tropopause at around altitude. This confirms that the Western Pacific region is dominant for the emergence of high δD(H_2O) values in the tropical lower stratosphere during JJA. The patch with negative values between 30°N and 50°N and 15 and suggests that the lack of the southward wind component in the American region, leaves more isotopically enriched water vapourat the higher altitudes of the American extratropics.~~

5.1 ~~Correlation analysis with Monsoon systems~~

~~In order to corroborate the hypothesis that ASM activity is crucial for the enhanced δD(H_2O) of the tropical tape recorder signal in JJA, a correlation analysis was carried out. For that, the anomalies w.r.t. the 21 year~~

average of the δD(H_2O) values between the 370 and the isentropes in the subtropical Western Pacific (15°N to 40°N and 120°E to 140°W) region and in the subtropical American and Western Atlantic region (15°N to 40°N and 120°W to 20°W) were correlated with the anomalies of the tropical δD(H_2O) may originate from in-mixing of old stratospheric air from the extratropics. Konopka et al. (2010) show a similar pattern for ozone which, according to Ploeger et al. (2012) , can also result in a stratospheric tape recorder signal in the stratosphere for the 21 years of the EMAC simulation. Fig. **??** shows the recorder-like signal. However, Ploeger et al. (2012) state that this process is largely dependent on the species itself, or more specifically, on its meridional gradient. The study shows that in-mixing plays a role for the annual ozone variations in the tropics, but not for carbon monoxide, nitrous oxide or water vapour. Another possible explanation for these patterns is the intrusion of tropospheric air into the stratosphere. Steinwagner et al. (2010) focus especially on slow ascent and dehydration through in situ cirrus formation which can generate the δD(H_2O) values averaged between the 370 and the isentropes and over the 21 years of the model simulation. The described regions are framed. The regions were selected to be north (15°N) of the tape recorder signal and below the altitude of its maximum, in order not to take the starting region of the tape recorder itself into account. A detailed description of the procedure and the applied Pearson's correlation is provided in the supplement.

δD(H_2O) between the 370 and the isentrope for JJA, averaged over the 21 years of the EMAC simulation. The frames mark the applied regions (black: ASM, blue: NAM) for the correlation analysis with the tape recorder signal.

The results are shown in Fig. **??**. Since the Monsoon signals for the correlation are taken from JJA, the time axes of the figures start in June. The tape recorder values for the correlation for the months of January to May are always taken from the subsequent year of the ASM signal.

Pearson's correlation coefficient between the δD(H_2O) tropical tape recorder signal and the δD(H_2O) ASM (left) and NAM (right) signal between the 370 and the isentrope for the 21 years of the EMAC simulation.

The left panel of Fig. **??** shows a tape recorder signal in the correlation coefficients of the ASM with the δD(H_2O) tape recorder signal. While in general this correlation shows values between −0.2 signal and 0.2, a stripe from in July to in April exhibits enhanced correlation values. The highest values, which reach a correlation of up to 0.7 can be seen from July to September between 18 and . In the following months this "correlation tape recorder" signal weakens with ascent over time and fades out in spring. The right panel of Fig. **??** shows the correlation coefficients between the NAM and the Randel et al. (2012) point out the importance of ice overshooting convetion on the pattern. In this section we will examine some of these mechanisms in order to obtain a better understanding of their relative importance on the δD(H_2O) tape recorder. Here, too, a "correlation tape recorder" signal can be detected, however, with slightly lower correlation coefficients, an earlier fade-out and especially, a smaller region of high correlation values during summer in the lower stratosphere. The spot between 22 and from July to October, with high correlation values is surprising and thought to be of different nature than the tape recorder signal. The ascent rate of the "correlation tape recorder" match with the ascent rate of the actual δD(H_2O) tape recorder. This correlation analysis confirms the connection between the strength of the Monsoon systems and the stratospheric tape recorder in δD(H_2O) and corroborates that the tropical δD(H_2O) signature in the stratosphere is closely related to the ASM.

6 The impact of ice lofting on stratospheric δD(H_2O)

5.1 In-mixing vs. lofted ice

Both, the water vapour mixing ratio and δD(H_2O), exhibit enhanced values in the lower stratosphere during JJA. The underlying processes for this, however, may differ in some ways for the two quantities. In order to demonstrate this, the water vapour mixing ratios and δD(H_2O) in the upper troposphere, lower stratosphere region (UTLS) in JJA are shown in Fig. 5.

H_2O mixing ratio (left panel) and δD(H_2O) (right panel) in the UTLS in JJA and tropopause height (black line), averaged over the 21 years of the EMAC simulation.

Differences in the distribution of the enhanced values can be observed when comparing the two panels. In the left panel, enhanced H_2O mixing ratios can be seen within almost the entire TTL, however, decreasing with altitude and towards the southern latitudes. At the northern edge of the TTL, the high H_2O mixing ratios exceed the tropopause and penetrate into the stratosphere. Some water vapour, however, also intrudes into the stratosphere in the central and the southern TTL. Isotopically enriched water vapour (see right panel) exclusively enters the stratosphere at the northern edge of the TTL. At first, we will examine if in-mixing of old stratospheric air from the extratropics alone can suffice to explain the δD(H_2O) values of around −600‰ can be observed, crossing the tropopause and entering the tropical pipe here. In the central and southern parts of the TTL, the water vapour is isotopically strongly depleted, exhibiting values below −700‰. Low) tape recorder. That water vapour from the extratropical stratosphere has been isotopically enriched through isotope effects during methane oxidation. These effects are relatively even throughout the year and broadly consistent with the chemical production rate of water vapour. A consistent relation between H_2O and δD(H_2O) values can be observed down to altitude in the central and southern TTL, while relatively high water vapour mixing ratios reach up to almost altitude in this region.

would therefore be expected, if in-mixing was the sole factor for this effect. In order to elucidate ~~this difference~~that this is not the case in the UTLS during JJA, the relation between the water vapour mixing ratios and ~~δD(H$_2$O)~~ its isotope ratio is presented in Fig. 7 for JJA and DJF. The black crosses denote this relation in the NH (~~10~~20°N and 40°N) and the red crosses in the ~~SH~~ Southern Hemisphere (SH) (40°S and ~~10~~20°S), both ~~in JJA~~ from 14 to 18 km.

~~The~~ In JJA, the red crosses can be found in a δD(H$_2$O) range between roughly ~~−720‰ and −640‰~~ −700‰ and −660‰ with water vapour mixing ratios of up to ~~. A slope~~ 10 μmol/mol. A relation of increasing δD(H$_2$O) with increasing ~~water vapour~~ H$_2$O mixing ratios is recognisable. The black crosses cover the range of the SH relations as well, but also spread out to ~~larger~~ higher water vapour mixing ratios and ~~larger~~ higher δD(H$_2$O) values. ~~Larger~~ Higher water vapour mixing ratios generally feature enhanced δD(H$_2$O) here ~~as well, but~~ too, but the black crosses are much wider distributed, especially for the same water vapour mixing ratios. In DJF, the black crosses cover roughly the range of the red crosses in JJA. The red crosses in DJF, however, hardly spread out to higher H$_2$O mixing ratios ~~as in the SH, some of the water vapour~~ and δD(H$_2$O), thus the relation differs only slightly between the hemispheres in DJF. The wider distribution of the relation between H$_2$O and δD(H$_2$O) in the NH ~~is isotopically enriched. This suggests that the processes , which elevate the water vapour in the respective hemispheres, differ. These are connected to convection and its influence on~~ during JJA suggests that several processes are being important here, because a single effect would lead to a rather compact picture in the H$_2$O to δD(H$_2$O) ~~through phase transitions.~~ relation. In particular, the combination of in-mixing of extratropical air and the intrusion of tropospheric air into the stratosphere are meant here. Crucial tropospheric processes are connected with cloud and convection effects partly in associacion with the monsoon systems. As mentioned above, upper tropospheric water vapour penetrating from the troposphere into the stratosphere could be crucial here. Also, the much discussed influence of ~~convectively lofted ice crystals (see e.g., Khaykin et al., 2009; Steinwagner et al., 2010; Bolot et al., 2013) is considered to be a major driver of~~ ice overshooting convection (see e.g., Khaykin et al., 2009; Bolot et al., 2013) may have a considerable effect on these patterns.

~~The~~ In order to provide a deeper insight into the ice water content and its isotopic signature, the mixing ratios of ice in the UTLS for JJA (left panel) and DJF (right panel) is shown in Fig. 8~~in order to reveal interhemispheric differences~~. Additionally, δD(ice) (the deuterium isotope ratio of the ice water content) is contoured in the figure and the height of the tropopause is marked. The white regions denote ice water mixing ratios below 0.1 μmol/mol.

The ice water mixing ratios in JJA show two local altitude maxima between roughly 12 and 15 km in this illustration. One in the inner tropics and another one between 30°N and 35°N. The latter maximum additionally features high δD(ice) at high altitudes up to the tropopause. Ice features δD values of up to −300‰ in this area, while the isotope ~~ratios~~ ratio of water vapour ~~lie~~ lies around −600‰ here (see Fig. 5). ~~Convectively lofted ice , which resublimates here, is therefore likely to~~ For DJF, a comparable maximum of lofted ice with high isotopic signatures at these latitudes (in the SH) is not simulated. Lofted ice which resublimates in the upper troposphere could therefore be responsible for the ~~isotopical~~ isotopic enrichment of water vapour in this region~~of the TTL. This water vapour hereafter intrudes~~ . The intrusion of this isotopically enriched water vapour into the tropical ~~stratosphere and generates the NH summer~~ pipe could then considerably amplify the δD(H$_2$O) tape recorder signal.

~~Regarding the analysis of the origin of the~~

5.2 Effects of convective and large-scale clouds

The possible influence of ice lofting into the upper troposphere and an associated isotopic enrichment of the tropical stratosphere during NH summer will be examined next. For this analysis, we carried out two additional sensitivity simulations with the EMAC model. Analogously to the additional simulation in Sect. 4 with a modified HDO tendency for methane oxidation, we now modified the HDO tendency for large-scale clouds (submodel: CLOUD) and for convection (submodel: CONVECT), respectively. These processes control ice lofting and its influence on δD(H$_2$O) in water vapour. Again, the tendency is modified in the manner that δD(H$_2$O) is not altered through the respective process. This enables us to assess the stratospheric δD(H$_2$O) patterns without the influence of each of these two processes and thus determine their respective contribution on the δD(H$_2$O) tape recorder. Since both of these processes almost exclusively operate in the troposphere, this analysis also allows the separation of the two above mentioned factors that are thought to control the δD(H$_2$O) tape recorder signal~~(Sect. 5) , the corresponding region where the ice lofting takes place is crucial. For this , the ice~~ : in-mixing of old stratospheric water vapour from the extratropics and the intrusion of tropspheric water vapour through the tropopause.

Analogue to Fig. 4, the annual amplitudes of δD(H$_2$O) as function of altitude are shown in Fig. 9. The black line denotes the standard simulation, the red line the simulation with modified HDO tendency for CLOUD and the green line with modified HDO tendency for CONVECT.

Around the tropopause, the amplitude of δD(H$_2$O) without the influence of large-scale clouds is smaller and the amplitude without the influence of convection is larger than in the standard simulation. This result is somewhat

~~Relation between H_2O and $\delta D(H_2O)$ from 14 to in JJA between 10°N and 40°N (black crosses) and between 40°S and 10°S (red crosses),~~

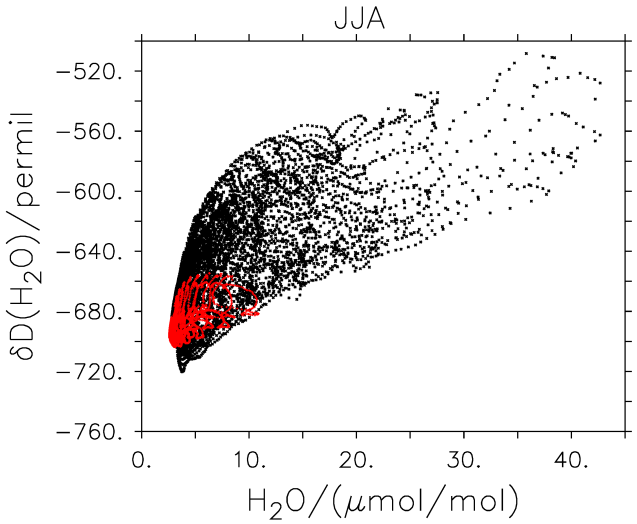

~~averaged over the 21 years of the EMAC simulation.~~

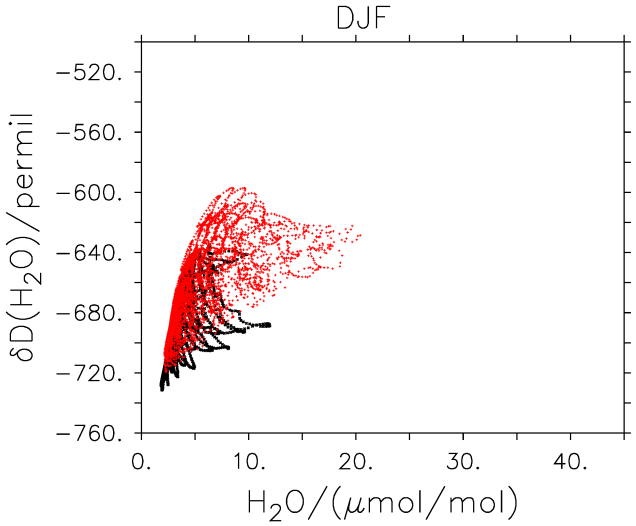

Fig. 7. Relation between H_2O and $\delta D(H_2O)$ from 14 to 18 km in JJA (left) and DJF (right) between 20°N and 40°N (black crosses) and between 40°S and 20°S (red crosses), averaged over the 21 years of the EMAC simulation.

surprising because in general, convection is thought to isotopically enrich water vapour, especially during JJA and therefore increase the annual $\delta D(H_2O)$ amplitude. In contrast, the stratosphere is generally isotopically enriched in this simulation compared to the standard simulation, which means that in our model, convection leads to isotopic depletion of the stratosphere. This is likely to be due to the underrepresentation of overshooting convection in the here applied convection scheme. Studies by Dessler et al. (2007) and Bolot et al. (2013) have shown that overshooting convection increases $\delta D(H_2O)$ in the UTLS. Instead, isotopic depletion through dehydration during the ascent of water vapour seems to dominate in the convection scheme. This process affects HDO stronger than H_2O and therefore leads to isotopic depletion. The tape recorder is somewhat more persistent in the upper parts because due to the generally higher stratospheric $\delta D(H_2O)$ values it is not affected as strongly by methane oxidation isotope effects.

The simulation without the effect of large-scale clouds shows a smaller $\delta D(H_2O)$ amplitude from the tropopause up to around 25 km. In other words, a weaker tape recorder with an earlier fade-out. The stratosphere is generally depleted compared to the standard simulation here and hence the chemistry affects the pattern more strongly. The smaller $\delta D(H_2O)$ amplitude below 25 km in this simulation shows that the isotopic enrichment during JJA is strongly influenced

~~Ice water content (colours) and δD(H_2O) in ice (dashed contour lines) in the UTLS in JJA and tropopause height (solid black line),~~

~~averaged over the 21 years of the EMAC simulation.~~

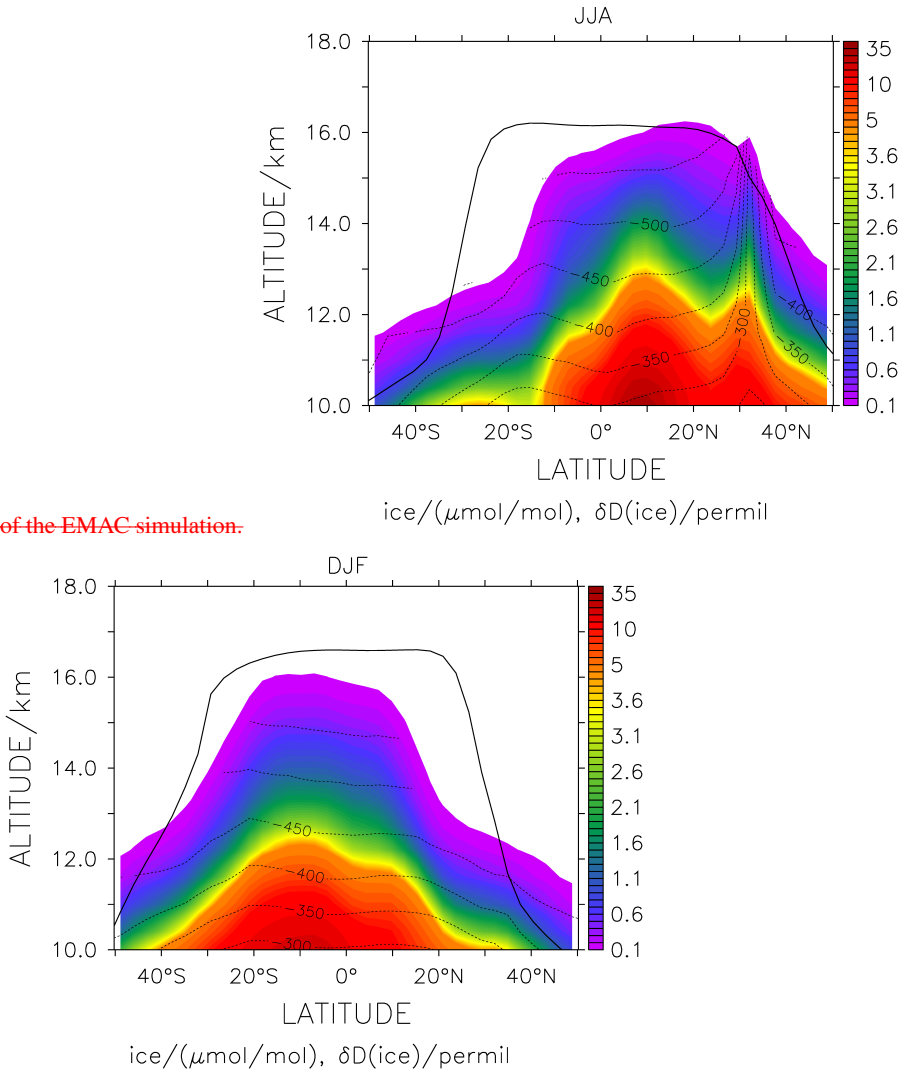

Fig. 8. Ice water content (colours) and δD(H_2O) in ice (dashed contour lines) in the UTLS in JJA (left) and DJF (right) and tropopause height (solid black line), averaged over the 21 years of the EMAC simulation. The white regions denote ice water mixing ratios below 0.1 $\mu mol \cdot mol^{-1}$.

through large-scale clouds. Hence, ice lofting and the isotopic enrichment of water vapour through resublimation are caused by large-scale clouds in our simulation. A possible mechanism for its influence on the tropical stratosphere will be presented in the following section. In conclusion, in-mixing of old stratospheric air from the extratropics alone can possibly generate a tape recorder-like signal for δD(H_2O), though, strong influences from tropospheric transport induced by large-scale and convective clouds do have a significant impact on the pattern.

5.3 A possible pathway through the tropopause

In order to depict a possible pathway of the isotopically enriched water vapour, which is complementing the δD(H_2O) tape recorder through the effect of ice lofting, the ice water content (left panel) and δD(ice) (right panel) in JJA at 14 km altitude are shown in Fig. 10. The altitude of 14 km was chosen because, as can be seen in Fig. 8, at this altitude the inner tropical and the northern subtropical altitude maxima of the ice water content are still pronounced. This provides information about the source of the influence of ice lofting on the δD(H_2O) tape recorder. Regions with ice water mixing ratios below 0.1 μmol/mol are again shaded white.

The left panel shows several spots of enhanced ice water mixing ratios around the convective zones in the trop-

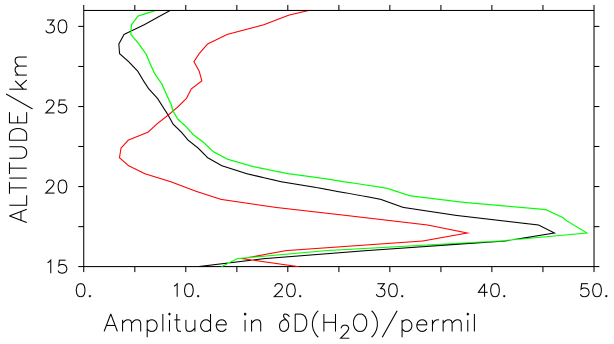

Fig. 9. Averaged annual amplitudes of δD(H_2O) with altitude, for the standard simulation (black), the simulation without large-scale cloud effect on δD(H_2O) (red) and the simulation without the effect of convection on δD(H_2O) (green).

ics. Especially, high ice water mixing ratios can be seen in Southeast Asia and Middle America, but by far the highest values are found over the Tibetan Plateau. δD(ice) exhibits a rather uniform picture around the tropics, with values mostly between $-500‰$ and $-400‰$. Only one single spot with isotopically enriched ice ~~water~~ above the Tibetan plateau with values above $-200‰$ strikes the eye. This corresponds with the latitude of the altitude maximum in Fig. 8 and ~~leads back to Sect. 5, where the origin of the NH summer signal of the~~ suggests that ice lofting over the Tibetan Plateau during the ASM season and associated isotopic enrichment of upper tropospheric water vapour can possibly account for the major part of this effect. The westerly wind regime in these latitudes (see Fig. 6) can transport the isotopically enriched water vapour from the continent over the West Pacific, where it can enter the stratosphere in the outflow of the ASM anticyclone. Here the tropopause is especially low and crossed by isentropic surfaces. The zonal cross section of δD(H_2O)~~tape recorder was traced back to the ASM. Convective activity over the~~ , averaged from 30°N to 40°N presented in Fig. 11 can provide additional evidence for this possible mechanism. Additionally, the tropopause and the isentropes are shown in the figure.

Here, the highest tropospheric δD(H_2O) values can be found at around 100°E i.e. above the Tibetan Plateau and ~~isotopic enrichment of upper tropospheric water vapour through exceptionally strong ice lofting, can therefore be understood as the starting point of the~~ corresponding with the ASM. Another, yet weaker, maximum lies at around 100°W which is the location of the Mexican High Plateau and the NAM. A third, even weaker maximum at 0°E can be associated with the North African Monsoon. The lowest values are found where the tropopause is highest, i.e., at around 16 km altitude at 50°E. This is also where the temperatures are lowest (not shown). The tropopause height exhibits two minima, one around 160°W and one around 10°W. Around these minima, the highest stratospheric δD(H_2O) ~~tape recorder in the EMAC simulation.~~ values are simulated. The underlying westerly wind regime (shown in Fig. 6) and the tropopause-crossing isentropes in the subtropics are thus supporting the suggestion of an ice lofting effect in association with the monsoon systems for the generation of the δD(H_2O) tape recorder.

6 Summary and discussion

As a first application of the new H2OISO submodel within the EMAC model, stratospheric water vapour isotope ratios were investigated. The time series of water vapour in the here ~~applied~~ analysed nudged EMAC simulation reproduces the major variations of the recent decades. The time series of δD(H_2O) shows similarities with H_2O, differs however, mainly regarding short term changes. This suggests that the processes controlling these two quantities coincide, but their effect on the respective value is of different quantity.

The impact of methane oxidation on the stratospheric δD(H_2O) tape recorder signal was ~~tested~~ investigated by comparing the evaluated EMAC simulation with an additional simulation ~~,~~ with a suppressed chemical ~~effect~~ isotope effect of methane oxidation on δD(H_2O). ~~The chemistry~~ Methane oxidation mainly affects water vapour and its isotopic signature above 25 km ~~,~~ where the δD(H_2O) tape recorder signal fades out faster through this chemical effect. Additionally, the amplitude of the δD(H_2O) tape recorder is reduced because methane oxidation influences the low δD(H_2O) values and the low water vapour mixing ratios stronger than the higher ones. This result is not surprising, however, it reveals the impact of the isotope chemistry on the tape recorder. Randel et al. (2012) also applied a correction for the methane effect on δD(H_2O) to the ACE-FTS satellite retrieval. This lead to the removal of the increase in δD(H_2O) with altitude in the stratosphere as well. Moreover, it generated enhanced isotope ratios in the lower stratosphere during JJA and SON, compared to without the methane correction. However, the δD(H_2O) tape recorder is still not clearly visible in the ACE-FTS satellite retrieval.

~~The signal~~ The determining processes for the generation of enhanced δD(H_2O) during JJA in the ~~lower stratosphere was traced back to its originating region and its determining process in the EMAC simulation. The main origin of the isotopically enriched water vapour during JJA in the lower stratosphere could be associated with the ASM. This water vapour originates from the Tibetan Plateau, crosses the tropopause over the Western Pacific and there, experiences southward transport at the forefront of the ASM anticyclone. The analysis of the correlation coefficient between the anomalies of the~~ tropical lower stratosphere were shown to take place exclusively in the NH. This is in contrast to water vapour itself, which is also influenced by direct transport through

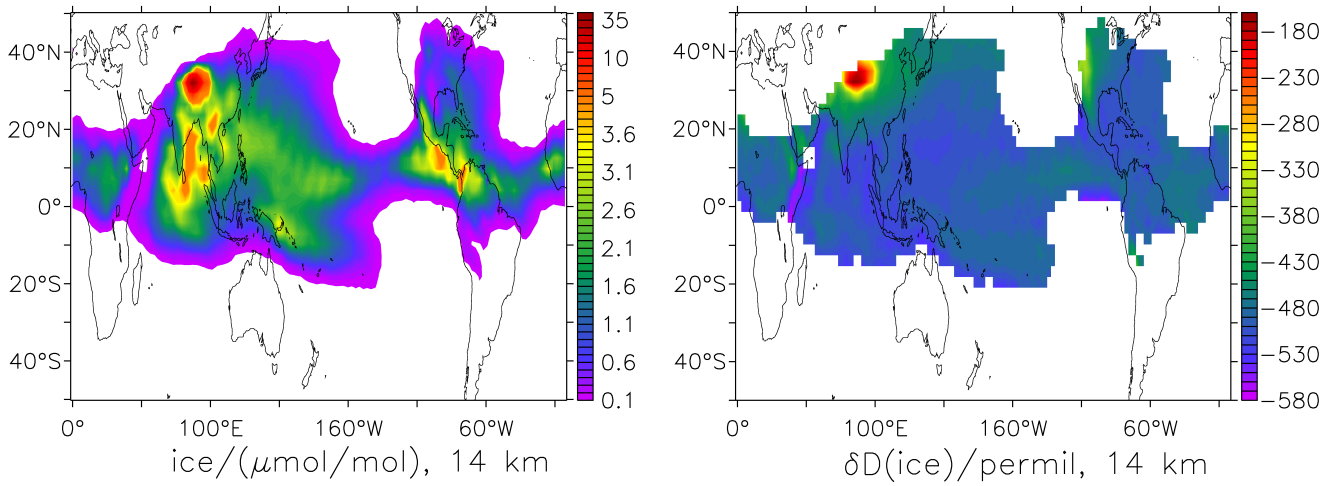

Fig. 10. Ice water content (left) and δD(ice) (right) at 14 km altitude in JJA, averaged over the 21 years of the EMAC simulation. The white regions denote ice water mixing ratios below 0.1 $\mu mol \cdot mol^{-1}$.

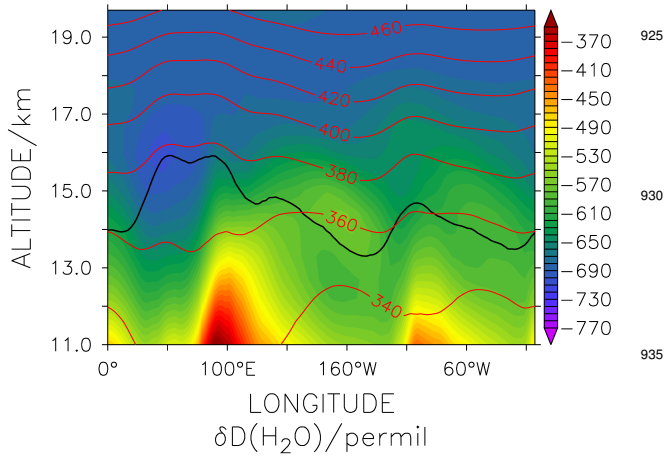

Fig. 11. Zonal cross section of δD(H_2O), averaged from 30°N to 40°N for JJA (averaged over the 21 years of the EMAC simulation). The black line denotes the tropopause height, the red contour lines indicate levels of constant potential temperatures (isentropes) in K.

the TTL (see e.g. also, Fueglistaler et al., 2004, 2009). Ploeger et al. (2012) showed that for some species a tape recorder-like signal can be generated through the in-mixing of old stratospheric air alone. However, e.g. Steinwagner et al. (2010) and Randel et al. (2012) focus mostly on slow ascent of tropospheric water vapour and convective ice overshooting when evaluating the reasons for the generation of the δD(H_2O) tape recorder. In order to investigate the role of the individual processes, we first assessed the H_2O to δD(H_2O) ~~values in the Monsoon regions and the tape recorder signal in~~ ratio in the different hemispheres and seasons. A much more spread H_2O to δD(H_2O) relation during JJA in the NH (compared to the SH and to DJF) suggested that both, intrusion of tropospheric water vapour and in-mixing of old stratospheric air are influencing δD(H_2O) ~~corroborated this connection. Furthermore, it supports the assumption, that the effect of the NAM on the tape recorder is smaller compared to the effect of the ASM. A link between the ASM and the tropical tape recorder in water vapour has already been found by Dethof et al. (1999). The southern flank of the anticyclone moistens the UTLS during JJA and contributes significantly to the stratospheric water vapour budget (see also Bannister et al., 2004; Gettelman and Kinnison, 2004; Lelieveld~~ ~~Also according to Fueglistaler et al. (2004) this side-ways transport into the tropics from the ASM complements the transport through the tropopause throughout the year~~here. In particular, due to extreme interhemispheric differences in the ice water content and its isotopic signature during the different seasons the lofting of ice crystals is assumed to enrich water vapour in the NH upper troposphere during JJA. Confirmation is achieved through the results of sensitivity simulations with modified HDO tendency for large-scale clouds and for convection, respectively. The averaged annual difference between the maximum and the minimum of δD(H_2O) shows a clear reduction in the UTLS up to 23 km for the simulation without large-scale clouds affecting δD(H_2O) and an enhancement for the simulation without convection affecting HDO. The isotopic enrichment during JJA is therefore not generated by convective events, which in contrast deplete the water vapour in the simulation, but by large-scale clouds in association with monsoon systems. However, ~~for~~ this shows that the δD(H_2O) tape recorder ~~, Steinwagner et al. (2010) suggest a slow dehydration by~~

~~cirrus clouds to have a key role by analysing MIPAS satellite data. The relative importance of the individual processes for the annual signal have thus to be further investigated.~~ is strongly controlled by tropospheric effects through clouds and convection and not simply by in-mixing of extratropical air masses.

Augmented ~~convective ice loftingduring the ASM season~~ ice lofting, especially in the ASM over the Himalaya mountains, has been shown to isotopically strongly enrich the water vapour in the upper troposphere. ~~Lateron, this~~ In the outflow of the monsoonal anticyclones this isotopically enriched water vapour is transported into the stratosphere on isentropic surfaces. Numerous studies (e.g. Bannister et al., 2004; Gettelman and Kinnison, 2004; Lelieveld et al., 2007; James et al., 2008) have shown that this side-ways transport into the tropics in particular from the ASM also contributes significantly to the stratospheric water vapour budget. Steinwagner et al. (2010) suggest a slow dehydration through cirrus cloud formation to have a key role for the δD(H_2O) tape recorder ~~in the EMAC simulation~~by analysing MIPAS satellite data. However, the separation of this particular process within the individual parts of the model, i.e. large scale and convective clouds, is not as easily resolvable. In the model, convective clouds isotopically deplete stratospheric water vapour. The relative importance of this individual process for the annual signal has to be further investigated, though. Randel et al. (2012) present a ~~different behaviour~~ somewhat different pattern of δD(H_2O) in the UTLS by analysing ACE-FTS satellite data. In this retrieval, enriched δD(H_2O) at 16.5 km altitude can ~~be found only~~ mostly be found over America and the patch of high δD(H_2O) associated with the ASM, as seen in the EMAC data is ~~entirely lacking~~considerably weaker. Convective ice overshooting is under discussion as to whether having a significant effect on the stratospheric water vapour budget ~~(see i.e. Khaykin et al., 2009)~~ (see e.g. Khaykin et al., 2009) . According to Dessler et al. (2007) and Bolot et al. (2013), however, it has a substantial effect on the stratospheric δD(H_2O) signature~~in the UTLS~~. This ice overshooting ~~effect performs~~ occurs mostly in the inner tropics and has the potential to isotopically enrich the tropical lower stratosphere. However, the NAM is also associated with strong convective ice overshooting ~~(Uma et al., 2014)~~ (see e.g., Uma et al., 2014) . The direct intrusion of ice crystals into the stratosphere ~~, though,~~ is known to be represented rather sparsely by the here applied convection scheme from Tiedtke (1989) ~~. Hence~~and has been shown to not affect stratospheric δD(H_2O) in this simulation. Therefore, this discrepancy between model and observations may be due to the underrepresentation of convective ice overshooting in the applied convection scheme. ~~The outstanding high isotopic signature in ice over Asia, may hence be an artefact of the underrepresented ice overshooting. The~~ The NAM region as well as the inner tropics ~~may posses comparably high~~ could show considerably higher δD(ice) values in the UTLS. ~~The estimate of the effect of the ASM region on stratospheric δD(H_2O) may therefore be distorted. Moreover~~Furthermore, this is ~~most likely~~ possibly also the cause for the too low δD(H_2O) values in the lower tropical stratosphere in EMAC compared to satellite observations during NH summer, as shown in the companion part 1 of this article (Eichinger et al., 2014). A more detailed evaluation of this effect can be conducted through the implementation ~~and application~~ of water isotopologues ~~in~~ into other convection schemes of EMAC. Future sensitivity studies can then also resolve the robustness of the here discovered patterns and possibly explain the differences between model results and observations more precisely.

7 Conclusions

The temporal variations of stratospheric δD(H_2O) reveal connections to those of water vapour~~. However, the changes show a different behaviour concerning~~ , however, show differences regarding the amplitudes. This provides additional information about the underlying processes of the changes and therefore can help to gain a better understanding of the reasons for the trends and variations of the stratospheric water vapour budget. Beforehand, this requires an understanding and quantification of the influence of the individual processes that are responsible for the patterns of δD(H_2O) in the stratosphere.

~~The isotope~~ Isotope fractionation effects during methane oxidation blur the δD(H_2O) tape recorder signal ~~,~~ by damping its amplitude and overshadowing it at higher altitudes. This explains the weaker tape recorder signal in δD(H_2O) compared to those in H_2O and HDO. ~~The origin of enhanced~~ In-mixing of old stratospheric water vapour with high isotope ratios from the extratropics alone does not suffice to describe the δD(H_2O) ~~in the lower stratosphere during NH summer in the EMAC model simulation was traced back to the Asian Summer Monsoon (ASM). Here, strong convection over the Tibetan Plateau lofts ice crystals into the upper troposphere, where these, when resublimating, isotopically enrich the water vapour~~ tape recorder. Instead, the influence of the intrusion of tropospheric water vapour through clouds and convection contribute significantly to this pattern. Isotopic enrichment of upper tropospheric water vapour through ice lofting in association with monsoon systems and further transport of these air masses into the tropical stratosphere in the outflow account for this influence. ~~This water vapour crosses the tropopause over the Western Pacific and furthermore, follows the monsoonal anticyclone into the tropics. This process was shown to significantly contribute to the δD(H_2O) tape recorder signal in the EMAC simulation.~~ However, a quantification of the contributions of the respective processes and also of the individual monsoon systems are yet to be established and first require further analyses of the discrepancies between the model results

and satellite retrievals~~indicate~~. These discrepancies indicate possible insufficiencies in the model, i.e. the underrepresentation of overshooting convection.

This study has set the basis for further analyses in order to determine the connection between the patterns and changes in stratospheric H_2O and $\delta D(H_2O)$. The additional information provided by the water isotope ratio ~~can be~~ is of significant support to unravel the factors ~~,~~ which contribute to trends and variations in the stratospheric water vapour budget.

Acknowledgements. The authors thank the DFG (Deutsche Forschungsgemeinschaft) for funding the research group SHARP (Stratospheric Change and its Role for Climate Prediction, DFG Research Unit 1095); the presented study was conducted as part of R. Eichingers PhD thesis under grant number BR 1559/5-1. We acknowledge support from the Leibnitz Supercomputing Center (LRZ), the German Climate Computing Center (DKRZ) and thank all MESSy developers and submodel maintainers for their support. Moreover, we thank H. Garny for an important impulse and S. Brinkop for important comments on the manuscript. Last but not least, we acknowledge the constructive comments of two anonymous referees helping to significantly improve this manuscript.

The service charges for this open access publication have been covered by a Research Centre of the Helmholtz Association.

References

Bannister, R. N., O'Neill, A., Gregory, A. R., and Nissen, K. M. (2004). The role of the south-east Asian monsoon and other seasonal features in creating the 'tape-recorder' signal in the Unified Model. *Quarterly Journal of the Royal Meteorological Society*, 130:1531–1554.

Bolot, M., Legras, B., and Moyer, E. (2013). Modelling and interpreting the isotopic composition of water vapour in convective updrafts. *Atmospheric Chemistry and Physics*, 13:7903–7935.

Dee, D. P., Uppala, S. M., Simmons, A. J., Berrisford, P., Poli, P., Kobayashi, S., Andrae, U., M. A. Balmaseda, M. A., Balsamo, G., Bauer, P., Bechtold, P., Beljaars, A. C. M., van de Berg, L., Bidlot, J., Bormann, N. B., Delsol, C., Dragani, R., Fuentes, M., Geer, A. J., Haimberger, L., Healy, S. B., Hersbach, H., Hólm, E. V., Isaksen, L., Kållberg, P., Köhler, M., Matricardi, M., McNally, A. P., Monge-Sanz, B. M., Morcrette, J.-J., Park, B.-K., Peubey, C., de Rosnay, P., Tavolato, C., Thépaut, J.-N., and Vitart, F. (2011). The ERA-Interim reanalysis: configuration and performance of the data assimilation system. *Quarterly Journal of the Royal Meteorological Society*, 656:553–597.

Dessler, A. E., Hanisco, T. F., and Füglistaler, S. (2007). Effects of convective ice lofting on H2O and HDO in the tropical tropopause layer. *Journal of Geophysical Research - Atmospheres*, 112(D18).

Dessler, A. E., Schoeberl, M. R., Wang, T., Davis, S. M., and Rosenlof, K. H. (2013). Stratospheric water vapor feedback. *PNAS*, 110:18087–18091.

Dessler, A. E. and Sherwood, S. C. (2003). A model of HDO in the tropical tropopause layer. *Atmospheric Chemistry and Physics*, 3:4489–4513.

Dethof, A., O'Neill, A., Slingo, J. M., and Smit, H. G. J. (1999). A mechanism for moistening the lower stratosphere involving the Asian summer monsoon. *Quarterly Journal of the Royal Meteorological Society*, 125:1079–1106.

Eichinger, R., Jöckel, P., Brinkop, S., Werner, M., and Lossow, S. (2014). Simulation of the isotopic composition of stratospheric water vapour – Part 1: Description and evaluation of the EMAC model. *Atmospheric Chemistry and Physics Discussion*, 14:23807–23846.

Forster, P. M. d. F. and Shine, K. P. (1999). Stratospheric water vapour changes as a possible contributor to observed stratospheric cooling. *Journal of Geophysical Research*, 26(21):3309–3312.

Fueglistaler, S., Dessler, A. E., Dunkerton, J. T., Folkins, I., Fu, Q., and Mote, P. W. (2009). Tropical Tropopause Layer. *Reviews of Geophysics*, 47:RG1004.

Fueglistaler, S., Wernli, H., and Peter, T. (2004). Tropical troposphere-to-stratosphere transport inferred from trajectory calculations. *Journal of Geophysical Research*, 109:D03108.

Gettelman, A. and Kinnison, D. E. (2004). Impact of monsoon circulations on the upper troposphere and lower stratosphere. *Journal of Geophysical Research*, 109:D22101.

Hagemann, R., Nief, G., and Roth, E. (1970). Absolute isotopic scale for deuterium analysis of natural waters. Absolute D/H ratio for SMOW. *Tellus*, 22:712–715.

Hagemann, S., Arpe, K., and Roeckner, E. (2006). Evaluation of the Hydrological Cycle in the ECHAM5 Model. *Journal of Climate*, 19:3810–3827.

Hegglin, M. I., Plummer, D. A., Shepherd, T. G., Scinocca, J. F., Anderson, J., Froidevaux, L., Funke, B., Hurst, D., Rozanov, A., Urban, J., von Clarmann, T., Walker, K. A., Wang, H. J., Tegtmeier, S., and Weigel, K. (2014). Vertical structure of stratospheric water vapour trends derived from merged satellite data. *Nature Geoscience*, 7:768–776.

Hoffmann, G., Werner, M., and Heimann, M. (1998). Water isotope module of the ECHAM atmospheric general circulation model: A study on timescales from days to several years. *Journal of Geophysical Research*, 103:16,871–16,896.

Hurst, D. F., Oltmans, S. J., Vömel, H., Rosenlof, K. H., Davis, S. M., Ray, E. A., Hall, E. G., and Jordan, A. F. (2011). Stratospheric water vapor trends over Boulder, Colorado: Analysis of the 30 year Boulder record. *Journal of Geophysical Research*, 116:D02306.

IAEA (2009). Reference Sheet for VSMOW2 and SLAP2 international measurement standards. *International Atomic Energy Agency*, Vienna:p. 5, URL: http://curem.iaea.org/catalogue/SI/pdf/VSMOW2_SLAP2.pdf.

James, R., Bonazzola, M., Legras, B., Surbled, K., and Fueglistaler, S. (2008). Water vapor transport and dehydration above convective outflow during Asian monsoon. *Geophysical Research Letters*, 35:L20810.

Jöckel, P., Kerkweg, A., Buchholz-Dietsch, J., Tost, H., Sander, R., and Pozzer, A. (2008). Technical Note: Coupling of chemical processes with the Modular Earth Submodel System (MESSy) submodel TRACER. *Atmospheric Chemistry and Physics*, 8:1677–1687.

Jöckel, P., Kerkweg, A., Pozzer, A., Sander, R., Tost, H., Riede, H., Baumgärtner, A., Gromov, S., and Kern, B. (2010). Development cycle 2 of the Modular Earth Submodel System (MESSy2). *Geoscientific Model Development*, 3:1423–1501.

Jöckel, P., Sander, R., Kerkweg, A., Tost, H., and Lelieveld, J. (2005). Technical Note: The Modular Earth Submodel System (MESSy), a new approach towards Earth System Modeling. *Atmospheric Chemistry and Physics*, 5:433–444.

Jöckel, P., Tost, H., Pozzer, A., Brühl, C., Buchholz, J., Ganzeveld, L., Hoor, P., Kerkweg, A., Lawrence, M. G., Sander, R., Steil, B., Stiller, G., Tanarhte, M., Taraborrelli, D., van Aardenne, J., and Lelieveld, J. (2006). The atmospheric chemistry general circulation model ECHAM5/MESSy1: consistent simulation of ozone from the surface to the mesosphere. *Atmospheric Chemistry and Physics*, 6:5067–5104.

Johnson, D. G., Jucks, K. W., Traub, W. A., and Chance, K. V. (2001). Isotopic composition of stratospheric water vapor: Implications for transport. *Journal of Geophysical Research*, 106:12219–12226.

Khaykin, S., Pommereau, J.-P., Korshunov, L., Yushkov, V., Nielsen, J., Larsen, N., Christensen, T., Garnier, A., Lukyanov, A., and Williams, E. (2009). Hydration of the lower stratosphere by ice crystal geysers over land convective systems. *Atmospheric Chemistry and Physics*, 9:2275–2287.

Konopka, P., Grooß, J.-U., Günther, G., Ploeger, F., Pommrich, R., Müller, R., and Livesey, N. (2010). Annual cycle of ozone at and above the tropical tropopause: observations versus simulations with the Chemical Lagrangian Model of the Stratosphere (CLaMS). *Atmospheric Chemistry and Physics*, 10:121–132.

Lelieveld, J., Brühl, C., Jöckel, P., Steil, B., Crutzen, J. P., Fischer, H., Giorgetta, M. A., Hoor, P., Lawrence, M. G., Sausen, R., and Tost, H. (2007). Stratospheric dryness: model simulations and satellite observations. *Atmospheric Chemistry and Physics*, 7:1313–1332.

Liu, Y. S., Fueglistaler, S., and Haynes, P. H. (2010). Advection-condensation paradigm for stratospheric water vapor. *Journal of Geophysical Research*, 115:D24.

Moyer, E. M., Irion, F. W., Yung, Y. L., and Gunson, M. R. (1996). ATMOS stratospheric deuterated water and implications for troposphere-stratosphere transport. *Geophysical Research Letters*, 23:2385–2388.

Niwano, M., Yamazaki, K., and Shiotani, M. (2003). Seasonal and QBO variations of ascent rate in the tropical lower stratosphere as inferred from UARS HALOE trace gas data. *JOURNAL OF GEOPHYSICAL RESEARCH*, 108:D24, 4794.

Nordeng, T. E. (1994). Extended version of the convection parameterization scheme at ECMWF and their impacts upon the mean climate and transient activity of the model in the tropics. *Res. Dep. Tech Memo*, 206:41 pp., Eur. Cent. for Medium–Range Weather Forecast, Reading, Berkshire, U.K.

Ploeger, F., Konopka, P., Müller, R., Fuelglistaler, S., Schmidt, T., Manners, J., Grooß, J., Günther, G., Forster, P., and Riese, M. (2012). Horizontal transport affecting trace gas seasonality in the Tropical Tropopause Layer (TTL). *Journal of Geophysical Research*, 117:D09303.

Plumb, A. R. (2002). Stratospheric Transport. *Journal of the Meteorological Society of Japan*, 80:793–809.

Randel, W. J. and Jensen, E. J. (2013). Physical processes in the tropical tropopause layer and their roles in a changing climate. *Nature Geoscience*, 6:169–176.

Randel, W. J., Moyer, E., Park, M., Jensen, E., Bernath, P., Walker, K., and Boone, C. (2012). Global variations of HDO and HDO/H_2O ratios in the upper troposphere and lower stratosphere derived from ACE-FTS satellite measurments. *Journal of Geophysical research*, 117:D06303.

Reid, G. C. and Gage, K. S. (1996). The tropical tropopause over the western Pacific: Wave driving, convection, and the annual cycle. *Journal of Geophysical Research*, 101:21,233–21,241.

Ridal, M., Jonsson, A., Werner, M., and Murtagh, D. P. (2001). A one-dimensional simulation of the water vapor isotope HDO in the tropical stratosphere. *Journal of Geophysical Research*, 106:32283–32294.

Ridal, M. and Siskind, D. E. (2002). A two-dimensional suimulation of the isotopic composition of water vapor and methane in the upper atmosphere. *Journal of Geophysical Research*, 107:D24,4807.

Rosenlof, K. H., Tuck, A. F., Kelly, K. K., Russel, J. M., and McCormick, M. P. (1997). Hemispheric asymmetries in water vapor and inferences about transport in the lower stratosphere. *Journal of Geophysical Research*, 102:13213–13234.

Schmidt, G. A., Hoffmann, G., Shindell, D. T., and Hu, Y. (2005). Modeling atmospheric stable water isotopes and the potential for constraining cloud processes and stratosphere-troposphere water exchange. *Journal of Geophysical Research*, 110:D21314.

Shindell, D. T. (2001). Climate and ozone response to increased stratospheric water vapor. *Geophysical Research Letters*, 28/8:1551–1554.

Steinwagner, J., Füglistaler, S., Stiller, G., von Clarmann, T., Kiefer, M., Borsboom, P.-P., van Delden, A., and Röckmann, T. (2010). Tropical dehydration processes constrained by the seasonality of stratospheric deuterated water. *Nature Geoscience*, 3(4):262–266.

Tiedtke, M. (1989). A comprehensive mass flux scheme for cumulus parameterization in large-scale models. *Monthly Weather Review*, 117:1779–1800.

Uma, K. N., Das, S. K., and Das, S. S. (2014). A climatological perspective of water vapor at the UTLS region over different global monsoon regions: observations inferred from the Aura-MLS and reanalysis data. *Climate Dynamics*, 42:10.1007.

Werner, M., Heimann, M., and Hoffmann, G. (2001). Isotopic composition and origin of polar precipitation in present and glacial climate simulations. *Tellus B*, 53B:53–71.

Werner, M., Langebroek, P. M., Carlsen, T., Herold, M., and Lohmann, G. (2011). Stable water isotopes in the ECHAM5 general circulation model: Toward high-resolution isotope modeling on a global scale. *Journal of Geophysical Research*, 116:D15109.

Zahn, A., Franz, P., Bechtel, C., Grooss, J., and Röckmann, T. (2006). Modelling the budget of middle atmospheric water vapour isotopes. *Atmospheric Chemistry and Physics*, 6:2073–2090.

Supplement of

Simulation of the isotopic composition of stratospheric water vapour – Part 2: Investigation of HDO/H_2O variations

R. Eichinger[1], P. Jöckel[1], and S. Lossow[2]

[1] Deutsches Zentrum für Luft- und Raumfahrt
Institut für Physik der Atmosphäre
Oberpfaffenhofen, 82230 Wessling, Germany

[2] Karlsruhe Institute of Technology
Institute for Meteorology and Climate Research
Hermann-von-Helmholtz-Platz 1, 76344 Leopoldshafen, Germany

Roland.Eichinger@dlr.de

Supplementary material for our article "Simulation of the isotopic composition of stratospheric water vapour – Part 2: Investigation of HDO/H_2O variations" in Atmos. Chem. Phys. (2014), available at: http://www.atmos-chem-phys.net

Date: April 21, 2015

Contents

1 Introduction

This supplement provides additional information to the article "Simulation of the isotopic composition of stratospheric water vapour – Part 2: Investigation of HDO/H_2O variations".

2 Combination of the satellite time series

2.1 Satellite data sets

The combined satellite time series is based on observations of the HALOE and MIPAS instruments.

HALOE was an instrument on UARS (Upper Atmosphere Research Satellite) providing data from September 1991 to November 2005. It employed the solar occultation technique measuring the attenuation of solar radiance during 15 sunrises and 15 sunsets per day. Based on the viewing geometry and the UARS orbit a latitudinal coverage between roughly 60°S and 60°N could be achieved within a month, while over a year the coverage extended from 80°S to 80°S. Water vapour results were retrieved from spectral information in the wavelength range between 6.54 μm and 6.67 μm (1500 cm^{-1} – 1528 cm^{-1}), typically in the altitude range from 10 km up to about 85 km (Russell et al., 1993). Here data from the retrieval version 19 are used (e.g. Randel et al., 2006; Scherer et al., 2008).

The MIPAS instrument was deployed on Envisat (Environmental Satellite) performing observations from 2002 to 2012. Different than HALOE the instrument measured the thermal emission at the atmospheric limb providing more than 1000 observations per day. Envisat used a polar, sun-synchronous orbit that allowed a latitudinal coverage from pole to pole on a daily basis (Fischer et al., 2008). The MIPAS data set is split into two parts due to an instrument failure in 2004. From 2002 to March 2004 MIPAS measured with its nominal resolution of 0.035 cm $^{-1}$ (designated as full resolution period – FR). Measurement recommenced in 2005 however with a reduced resolution of 0.0625 cm^{-1} (reduced resolution period – RR). For the combined satellite time series MIPAS data retrieved with the IMK/IAA (Institut für Meteorologie und Klimaforschung in Karlsruhe, Germany / Instituto de Astrofísica de Andalucía" in Granada, Spain) processor are used, i.e. versions 20 (FR) and 220/221 (RR). For both periods the water vapour information is retrieved from a dozen of microwindows distributed over the wavelength range between 7.09 μm and 12.57 μm (795 cm $^{-1}$ – 1411 cm^{-1}) covering the altitude range from about 10 km to the lower mesosphere.

2.2 Combination of the satellite data sets

The combination of the satellite data sets requires a handling of the biases that exist among them (Milz et al., 2009). For that in a first step monthly zonal means of the individual data sets are derived. In a second step the MIPAS data are adjusted towards HALOE by a scalar, time independent shift S that minimises the offset between both data sets in the overlap period in a root mean square sense:

$$RMS = \sqrt{\frac{1}{n} \cdot \sum_{i=1}^{n} \left[x_{i,H} - (x_{i,M} + S)\right]^2} \tag{1}$$

Here $x_{i,H}$ and $x_{i,M}$ denote the individual overlapping data points for HALOE and MIPAS and n describes the their total number. The shift S_{opt} that minimises Eq. 1 is given by:

$$S_{opt} = \frac{1}{n} \cdot \sum_{i=1}^{n} (x_{i,H} - x_{i,M}) \tag{2}$$

In a last step the overlapping HALOE and shifted MIPAS data points are averaged using their associated standard errors w_i from the monthly and zonal mean derivation as weights.

$$x_i = \frac{w_{i,H} \cdot x_{i,H} + w_{i,M} \cdot (x_{i,M} + S_{opt})}{w_{i,H} + w_{i,M}} \tag{3}$$

Figure 1 shows an example for the latitude range between 10°S and 10°N at an altitude of 25 km. In the upper panel the monthly zonal mean time series of HALOE is shown by the black line. The original MIPAS time series are given in blue. Both, for the full and reduced resolution period, the MIPAS data show higher volume mixing ratios than HALOE, as expected from earlier assessments (e.g. Kley et al., 2000; Milz et al., 2009). This aspect has to be taken into account when comparing the combined time series to other data sets. The adjusted MIPAS time series are shown in green and the final combined time series is shown in red. The lower panel shows the root mean square of the offset between HALOE and MIPAS in the overlap periods as function of the MIPAS shift S according to Eq. 1. The optimal shift S_{opt} of the MIPAS time series is indicated by the dashed line. For the full resolution period (black) the optimal shift is 0.43 ppmv and for the reduced resolution (grey) it is 0.33 ppmv. Overall, the shifts for both MIPAS periods are very similar as function of altitude and latitude (not shown here).

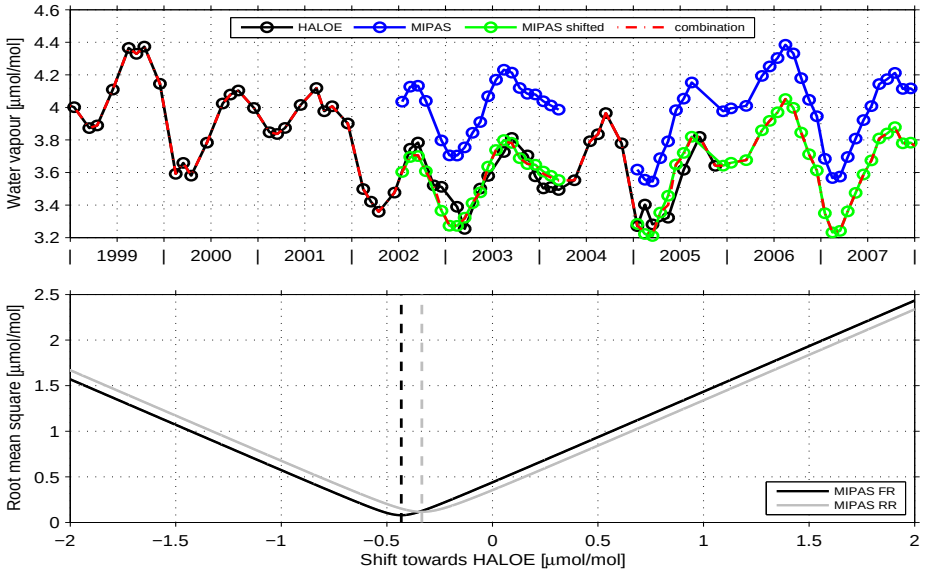

Figure 1: Example of the satellite data combination considering the zonal mean between 10°S – 10°N at 25 km. The upper panel shows the monthly mean HALOE and MIPAS time series in black and blue, respectively. The green line depicts the adjusted MIPAS time series and the combined time series is given by the red dash-dotted line. The lower panel shows the relationship between the shift of the MIPAS time series and the root mean square of the offset towards HALOE for the full (black) and reduced resolution period (grey) of MIPAS. The optimal shift of the MIPAS time series is indicated by the dashed lines.

3 Description of the modified chemical tendency of HDO

Here, we describe the modification of the additional EMAC simulation, applied for the investigation of the influence of methane isotope effects on the stratospheric δD(H_2O) tape recorder in Sect. 4. From the simulation described in Sect. 3, it differs in only one point: The calculation of the **c**hemical contribution to the tendency of HDO ($\frac{\partial(HDO)}{\partial t}|_C$) was implemented in a different manner. With the aim to suppress the influence of the chemistry on δD(H_2O), in a sensitivity simulation, the following approach was introduced:

$$\delta D'_a(H_2O) = \delta D_b(H_2O). \tag{4}$$

Here $\delta D'_{ac}(H_2O)$ represents the modified δD(H_2O) value **a**fter the addition of the chemical tendencies of HHO and HDO to their total tendencies and $\delta D_{bc}(H_2O)$ stands for δD(H_2O) **b**efore this operation. In order to fulfil this condition, a modified calculation of the chemical HDO tendeny was implemented into the H2OISO submodel. Considering the δ-notation

$$\delta D(H_2O) = \frac{R_{sample} - R_{VSMOW}}{R_{VSMOW}} \cdot 1000 = \left(\frac{R_{sample}}{R_{VSMOW}} - 1\right) \cdot 1000, \tag{5}$$

where R denotes the ratio of HDO to H_2O of the respective compound, Eq. 4 gives

$$\left[\frac{\left(HDO + \frac{\partial(HDO)}{\partial t}|_T \cdot \Delta t + \frac{\partial(HDO)}{\partial t}|_{C'} \cdot \Delta t\right)}{HHO + \frac{\partial(HHO)}{\partial t}|_T \cdot \Delta t + \frac{\partial(HHO)}{\partial t}|_C \cdot \Delta t} - 1\right] \cdot 1000 = \left[\frac{\left(HDO + \frac{\partial(HDO)}{\partial t}|_T \cdot \Delta t\right)}{HHO + \frac{\partial(HHO)}{\partial t}|_T \cdot \Delta t} - 1\right] \cdot 1000, \tag{6}$$

with $\frac{\partial(HDO)}{\partial t}|_T$ and $\frac{\partial(HHO)}{\partial t}|_T$ denoting the **t**otal tendencies before the addition of the chemical tendencies for the HDO and the HHO tracer, respectively. $\frac{\partial(HDO)}{\partial t}|_C$ stands for the chemical tendency of the HHO tracer and $\frac{\partial(HDO)}{\partial t}|_{C'}$ for the modified chemical tendency of the HDO tracer. HDO and HHO represent the $t-1$ values of the respective tracers and Δt the time step. Solving Eq. 6 for $\frac{\partial(HDO)}{\partial t}|_{C'} \cdot \Delta t$ leads to

$$\frac{\partial(HDO)}{\partial t}|_{C'} \cdot \Delta t = HHO + \frac{\partial(HHO)}{\partial t}|_T \cdot \Delta t - HDO - \frac{\partial(HDO)}{\partial t}|_T \cdot \Delta t \frac{HDO + \frac{\partial(HDO)}{\partial t}|_T \cdot \Delta t}{HHO + \frac{\partial(HHO)}{\partial t}|_T \cdot \Delta t} \tag{7}$$

for the modified chemical tendency of HDO. This modified chemical HDO tendency is always consistent with the chemical tendency of HHO, but δD(H_2O) does not become influenced by methane oxidation. In other words, in this sensitivity simulation, CH_4 and CH_3D have the same life times. This calculation can provide insight into the sensitivity of stratospheric δD(H_2O) patterns (e.g. the tape recorder) on the oxidation of CH_4 and CH_3D.

4 ~~The applied Pearson's correlation~~

~~The correlations were calculated by using one δD(H_2O) value per year for the respective (American and Asian) Monsoon activity (the average over JJA in the described regions, hereafter called P) and the δD(H_2O) value at every altitude level for each month per year (hereafter called Q). For these values, the Pearson's correlation coefficient $\rho(P,Q)$ is determined by~~

$$\rho(P,Q) = \frac{cov(P,Q)}{\sigma(P)\,\sigma(Q)} =$$

$$\sqrt{E\left[(P-\mu(P))^2\right]}\sqrt{E\left[(Q-\mu(Q))^2\right]},$$

~~where cov represents the covariance, σ the standard deviation, E the expectation and μ the mean.~~

4 Additional images

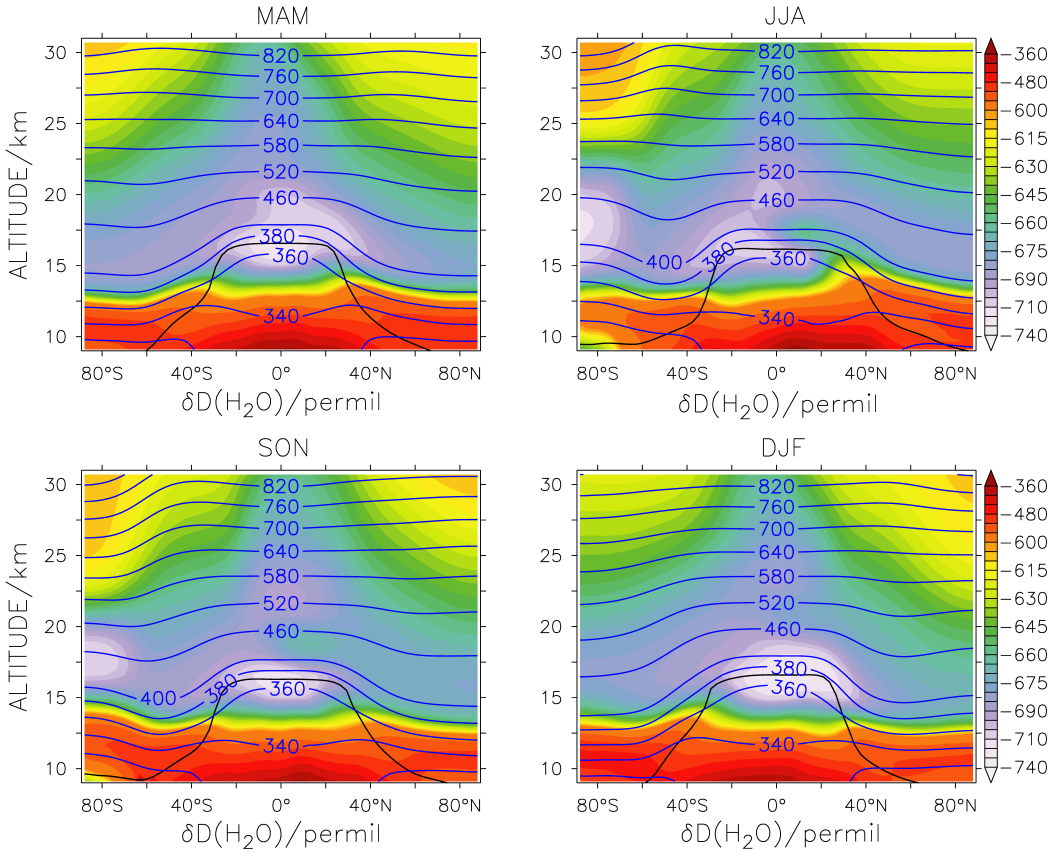

Figure 2: Zonally and seasonally averaged δD(H_2O) (coloured), tropopause height (black lines) and isentropes (blue contour lines) in K, averaged over the 21 years of the EMAC simulation. MAM: March, April, May; JJA: June, July, August; SON: September, October, November; DJF: December, January, February.

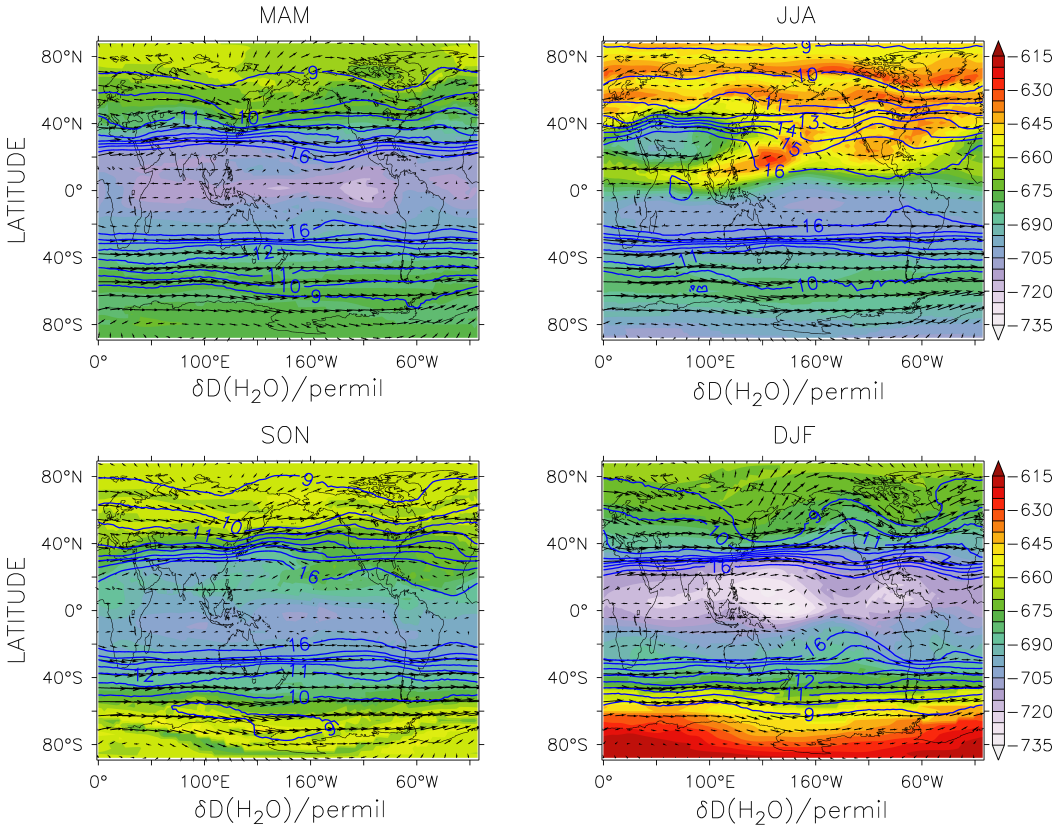

Figure 3: Seasonally averaged δD(H_2O) (colours), horizontal wind vectors (arrows) averaged from the 380 to the 400 K isentrope and the tropopause height (blue contour lines), averaged over the 21 years of the EMAC simulation. MAM: March, April, May; JJA: June, July, August; SON: September, October, November; DJF: December, January, February.

References

Fischer, H., Birk, M., Blom, C., Carli, B., Carlotti, M., von Clarmann, T., Delbouille, L., Dudhia, A., Ehhalt, D., Endemann, M., Flaud, J. M., Gessner, R., Kleinert, A., Koopman, R., Langen, J., López-Puertas, M., Mosner, P., Nett, H., Oelhaf, H., Perron, G., Remedios, J., Ridolfi, M., Stiller, G. P., and Zander, R.: MIPAS: An instrument for atmospheric and climate research, Atmospheric Chemistry & Physics, 8, 2151 – 2188, doi:10.5194/acp-8-2151-2008, 2008.

Kley, D., Russell, J. M., and Philips, C.: Stratospheric Processes and their Role in Climate (SPARC) - Assessment of upper tropospheric and stratospheric water vapour, SPARC Report 2, WMO/ICSU/IOC World Climate Research Programme, Geneva, 2000.

Milz, M., Clarmann, T. V., Bernath, P., Boone, C., Buehler, S. A., Chauhan, S., Deuber, B., Feist, D. G., Funke, B., Glatthor, N., Grabowski, U., Griesfeller, A., Haefele, A., Höpfner, M., Kämpfer, N., Kellmann, S., Linden, A., Müller, S., Nakajima, H., Oelhaf, H., Remsberg, E., Rohs, S., Russell, III, J. M., Schiller, C., Stiller, G. P., Sugita, T., Tanaka, T., Vömel, H., Walker, K., Wetzel, G., Yokota, T., Yushkov, V., and Zhang, G.: Validation of water vapour profiles (version 13) retrieved by the IMK/IAA scientific retrieval processor based on full resolution spectra measured by MIPAS on board Envisat, Atmospheric Measurement Techniques, 2, 379 – 399, 2009.

Randel, W. J., Wu, F., VöMel, H., Nedoluha, G. E., and Forster, P.: Decreases in stratospheric water vapor after 2001: Links to changes in the tropical tropopause and the Brewer-Dobson circulation, Journal of Geophysical Research, 111, D12 312, doi:10.1029/2005JD006744, 2006.

Russell, J. M., Gordley, L. L., Park, J. H., Drayson, S. R., Hesketh, W. D., Cicerone, R. J., Tuck, A. F., Frederick, J. E., Harries, J. E., and Crutzen, P. J.: The Halogen Occultation Experiment, Journal of Geophysical Research, 98, 10 777 – 10 797, 1993.

Scherer, M., Vömel, H., Fueglistaler, S., Oltmans, S. J., and Staehelin, J.: Trends and variability of mid-latitude stratospheric water vapour deduced from the re-evaluated Boulder balloon series and HALOE, Atmospheric Chemistry & Physics, 8, 1391 – 1402, doi:10.5194/acp-8-1391-2008, 2008.

Reply to referee #1

GENERAL REMARKS

- *this is a nice study evaluating a global climate model with isotopic fractionation for HDO. The goal of the manuscript is to better understand the mechanisms by which air gets into the stratosphere. The paper in its present form is only partially successful in this regard. It needs major revisions to be publishable in ACP. The sensitivity study of methane effects is good. My general critique of the manuscript is two fold. First, the description of monsoon impacts is confusing, and second the summary is more confusing with a discussion of lofted ice. I think the authors should think about a sensitivity study to remove the isotopic effects of lofted ice to prove their point. I think a further sensitivity study of lofted ice effects on delD could be conducted to clarify this: perhaps both globally and over the ASM region: lofted ice delD could just be set to the environmental delD to remove any lofted ice effect, and then differences performed.*

  Thank you for your valuable comments and suggestions. Please find below our reply to your specific points.

SPECIFIC COMMENTS

- Page 29460 L8: *no comma necessary*

  1. Thank you, will be corrected.

- Page 29460 L13: *effects...have a damping....(plural)*

  2. Thank you, will be corrected.

- Page 29463 L23: *can you add a sentence on how realistic the energy budget and hydrologic cycle is relative to observations? Nudged climate models need not represent reality very well. This is probably in the other paper, but please state here.*

  3.1 Hydrological cycle: The hydrological cyle of the basemodel ECHAM5 has been evaluated e.g. in Hagemann et al. (2006). Jöckel et al. (2006) state that the modifications introduced by the MESSy system, as well as by the application of the

T42L90MA resolution and nudging, produces a hydrological cycle similar to the results by Hagemann et al. (2006) and consistent with observations. With respect to the water isotopologues, this has indeed been done extensively in Part 1 of the article. We will include some sentences with additional references in the revised manuscript.

3.2 Energy budget: Yes, "nudging" changes the energy budget of the model (e.g. through clouds). However, the nudging applied here does not include "wave zero" in the spectral space (i.e., it is applied without "nudging" the global mean temperature), which minimises this effect. The reason to "nudge" the model for the present study was to achieve a representation of the interannual variation in dynamics (e.g., w.r.t. ENSO, NAO etc.) which is as realistic as possible to be able to compare directly with observations.

- Page 29464 L22: *for figure 1, what is the correlation coefficient?*

  4. Thank you, we forgot that, the (Pearson's) correlation between HALOE/MIPAS and EMAC is R^2=0.502. We will include it.

- Page 29465 L5:*determining : not proper grammar. "Both determined by Tropospehere-stratosphere exchange processes" would be better*

  5. Thanks for reading carefully, will be corrected

- Page 29465 L9:*is anticorrelated (not opposing).*

  6. Thanks, will be corrected

- Page 29466 L25: *I do not think the tape recorder figures are helpful : you could remove figure 3 & 4 and just show figure 5.*

  7. We disagree on that point. The tape recorder figures nicely show that the earlier fade-out of the δD(H_2O) tape recorder (compared to the H_2O tape recorder) is due to chemical isotope effects. This is particularly interesting as a follow-up for the studies in the companion paper (Part 1) and is not obvious from figure 5 only. Moreover, they show more clearly that in the upper levels the high δD(H_2O) values show a QBO signal and that this signal disappears in the second simulation. Therefore, we prefer to keep these images.

- Page 29467 L15: *affected more strongly*

  8. Thank you, we will correct that.

- Page 29470 L5: *but lower temps would imply more negative DelD.*

  9. Please see 13

- Page 29470 L11: *but the rest of the hemisphere also has relatively high delD at these altitudes and latitudes: could it be that the ASM is just making a region of low delD on a high delD background because it is warmer?*

  10. Please see 13

- Page 29470 L16: but these two monsoons have very different structures and water vapor signals : I believe randel and park among others deal with this. I do not think simple averages can be compared in this way.

  11. Thank you, among other issues, this leads us to delete the image, please also see 13

- Page 29470 L25: but the earlier figure shows that the high values are adjective from the lower stratosphere around the ASM anti-cyclone. Would that not be the cause?

  12. Please see 13

- Page 29472 L7: to me they look pretty similar up to 23 km or so. I do not think this supports the argument that one is more influential than the other: they are similar. Also: you correlate the NAM over the anticyclone with the ASM downstream.

  13. Thank you, these are important points.
  Considering this and also the comments of the second referee we decided to restructure Sects. 5 and 6:
  We will remove large parts of Sect. 5, including Fig. 9 and the entire Sect. 5.2. Instead, we will include an analysis of cloud and convection effects on the δD(H_2O) tape recorder based on additional sensitivity simulations. The main question addressed in this section will then no longer be the influences of the two monsoon systems, but rather if the in-mixing (of old stratospheric air) or the cloud/convective effects are (to what extent) responsible for the δD(H_2O) tape recorder. The question about the role of the two different monsoon systems, however, will still be addressed in the analysis and the revised discussion.
  Due to the interhemispheric differences of lofted ice and its influence on δD(H_2O) in stratospheric water vapour, the ice lofting analysis (Sect. 6) will be used as motivation at the start of the section.

- Page 29473 L16: *please explain here the mechanism: does this mean there is more lofted ice in the N hemisphere. I also think and analysis of DJF would be useful to see if the asymmetry holds in the cold season with low delD (large depletion).*

  14. Yes, there is more lofted ice in the NH. That is due to the greater land mass and hence stronger convection plus the monsoon systems. The figures below for DJF (13 and 14) support this point. Here, these patterns can not be observed. We will add these Figs. and clarify the analysis.

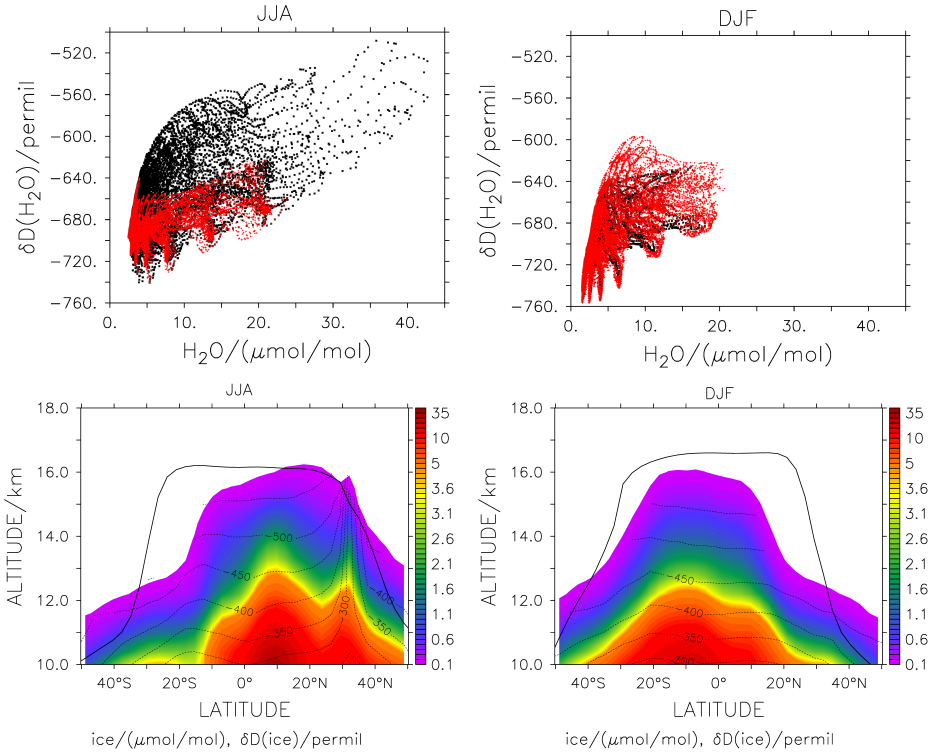

- Page 29474 L19: *the enhancement is at 18 km in figure 12. Does convection in the model penetrate to this altitude? You must have some convective mass flux output from the model available. What can you say about the relative mass of ice injected from delD?*

  15. No, convection does not penetrate up to 18 km in the model, it rather stays below the tropopause. The isotopical enrichment of water vapour due to convection is basically limited to the upper troposphere. However, this isotopically enriched water vapour is then further transported (monsoon outflow and isentropic transport) into the tropical stratosphere. The enhancement (that blob) at 18 km in Fig. 12 you are referring to, is a (maybe misleading) artefact, caused by the seasonal averaging. The mass of ice injected directly into the stratosphere is extremely low, but a slight increase would have a large effect on δD(H_2O). Thus, more ice injection in the model would produce results closer to observations (see Part 1). Hence the conclusion that the convection scheme may be responsible for the appearing differences between model and observations (later on). We will revise the text and add explanations in order to eliminate the causes for these misunderstandings.

- Page 29476 L7: *but you just said it was due to horizontal transport, and now it is due to ice lofting? I think a bit more analysis is warranted here. Or clarification, it sounds like you are talking about the same region.*

  16. Water vapour is isotopically enriched through convective ice lofting during the monsoon season, but only up to the upper troposphere (at least in the model).

From here on, monsoonal outflow and isentrope parallel transport is responsible for the advection of this isotopically enriched water vapour into the tropical stratosphere, where it experiences vertical transport. We will add a sentence to make this transport connection clear.

- Page 29476 L22: *how do you NSNOW the convection scheme is in error. You are discussing discrepancies with observations: please show the discrepancies.*

  17. Indeed we do not have proof for that. Here we refer to Fig. 11 in Randel et al. (2012). Together with the other cited studies this leads to these assumptions. We will revise the text and clarify that this "could" be an explanation

- Page 29477 L3: *since you have done this for methane HDO sources, I was expecting you to do the same thing for convective HDO: why not run a sensitivity test to determine what the lofted ice does to HDO? You could revert ice coming out of convection to the environment, and that would allow you to discern the signal.*

  18. Thank you very much for this suggestion. Instead of Sect. 5.2 we will now include an additional analysis, please see Point 13.

References

- Hagemann, S., Arpe, K., and Roeckner, E.: Evaluation of the hydrological cycle in the ECHAM5 model, J. Climate, 19, 38103827, 2006.

- Jöckel, P., Tost, H., Pozzer, A., Brühl, C., Buchholz, J., Ganzeveld, L., Hoor, P., Kerkweg, A., Lawrence, M. G., Sander, R., Steil, B., Stiller, G., Tanarhte, M., Taraborrelli, D., van Aardenne, J., and Lelieveld, J.: The atmospheric chemistry general circulation model ECHAM5/MESSy1: consistent simulation of ozone from the surface to the mesosphere, Atmos. Chem. Phys., 6, 50675104, 2006

Reply to referee #2

GENERAL COMMENT

- *This paper uses the EMAC model with a new submodel for calculating the water isotopologue HDO to investigate those processes determining the stratospheric water isotope composition and the water vapor budget. Particular emphasis is laid on understanding the tape recorder in δD. The authors present an interesting analysis of the effects of methane oxidation, which are shown to damp the δD-tape recorder above about 20 km. Further, they relate the summertime maximum of δD in the tropical lower stratosphere to transport processes in the Asian monsoon (ASM). Overall, this well written paper presents interesting results useful for deepening our understanding of stratospheric water vapor and I recommend publication. However, I have one major comment (specific comment 1) and a few minor comments which the authors need to address. Specific*

  Thank you very much for your interesting and helpful comments. Please find our answers to all your comments below.

SPECIFIC COMMENTS

- *1) Asian monsoon effect - convection or in-mixing:*

  My major comment concerns the interpretation of the summertime maximum of δD in the tropical lower stratosphere and the proposed relation to the Asian monsoon, as formulated e.g. in the conclusions P29477/L14ff (and similarly in other parts of the paper):

  The origin of enhanced $\delta D(H2O)$ in the lower stratosphere during NH summer in the EMAC model simulation was traced back to the Asian Summer Monsoon (ASM). Here, strong convection over the Tibetan Plateau lofts ice crystals into the upper troposphere, where these, when resublimating, isotopically enrich the water vapour. This water vapour crosses the tropopause over the Western Pacific and furthermore, follows the monsoonal anticyclone into the tropics. This process was shown to significantly contribute to the $\delta D(H2O)$ tape recorder signal in the EMAC simulation.

I have serious doubts concerning this interpretation which is, in addition, in contradiction to the interpretation given by Randel et al. (2012), that convective ice lofting in the American monsoon causes the summertime δD maximum.

1.1. This is an interesting and important point. The discrepancy between the conclusions (NAM vs. ASM) of Randel et al. (2012) and the present study arises from our results. We do discuss this discrepancy, which leads us to the argument, that the convection scheme might be in error. We will discuss this point much more thouroughly in the revised manusctipt, please see below.

If convection over Tibet enhances δD, why is δD above Tibet in the 380-400K layer particularly low (see Fig. 7)? The authors show that δD above Tibet is enhanced at 14 km, but how is this air of elevated δD transported upward, if not in the Asian monsoon?

1.2. But Fig. 8 shows that in the region where enriched tropospheric δD can be found, also the tropopause and the isentropes are elevated. The upward transport of the enriched air is indeed caused by the ASM, in the outflow. Isentropic transport in combination with the westerlies here can account for the advection to the region over the West Pacific, where the tropopause is low. Also for the NAM this can be seen, but weaker. However, for the West Pacific, this can be complemented by inflow from old stratospheric air from the extratropics, as you state below. We will discuss this point, please see below.

Remarkably, the tongue of enhanced δD air above the West Pacific (Fig. 7), which the authors relate to convection over Tibet, is also evident in distributions of stratospheric tracers like ozone, and has recently been linked to in-mixing of aged stratospheric air from the extratropics into the TTL (Konopka et al., 2010). This in-mixing causes the summertime maximum of ozone in the TTL. Ploeger et al. (2012) further discussed how a tape recorder signal can emerge from this in-mixing. In my opinion, Fig. 7 suggests a similar mechanism for creating the elevated δD values in the tropics around 18 km/15°N (Fig. 6). From this point of view, in-mixing of aged stratospheric air from the extratropics around the Asian monsoon anticyclone enhances the δD in the tropics, in EMAC.

1.3. Thank you for this important information. Indeed we did not consider this process sufficiently. We will discuss it in more detail in the revised manuscript. However, we are not convinced that a comparison with ozone would hold for this, since this in-mixing process is largely dependent on the species itself, more specifically on its meridional gradient. Ploeger et al., (2012) also state that this process plays a role for the annual ozone variation in the tropics, but not for carbon monoxide and water vapour. Moreover, as stated above, these processes do not exclude each other. The question will then be how large the respective contributions are for δD(H_2O).
We will perform an additional sensitivity study without the influence of cloud/ convection on δD(H_2O) in order to resolve this issue, and replace the correlation analysis in Sect. 5.2. In fact, this leads to a restructuring of Sects. 5 and 6, please

see below and also our answer to referee #1.

In addition, convective ice lofting likely plays a role in the American monsoon (NAM), as proposed by Randel et al. (2012). The authors state on P29476/L21 that these effects of deep convection are likely underrepresented in EMAC. Hence, it seems not clear to me which effect (NAM convection or ASM in-mixing) dominates in the atmosphere.

1.4. This is indeed one of the main questions remaining from this study. We suggest this to be investigated by implementing and using other convection schemes in future studies.

I think a correct interpretation and clear description of these effects is a key point of the paper and therefore additional analysis is needed to either (i) confirm the proposed effect (convection over Tibet) and present a counter-proof for my contrasting interpretation (ASM in-mixing), or (ii) correct the interpretation, or at least (iii) discuss the potentially involved mechanisms adequately. Perhaps an investigation of the correlation between δD and a stratospheric tracer like ozone (which is probably included in the simulation) in the Western Pacific region (co-located with the tongue of enhanced δD) and in the NAM could elucidate these points.

1.5. Thank you very much. We agree that our analysis was a bit weak in this respect and that the conclusions might go too far. Therefore we will restructure Sects. 5 and 6.
As also stated in the reply to referee #1, we will remove large parts of Sect. 5 (including Fig. 9) and subsection 5.2. Instead, we will investigate more deeply the role of cloud/convective effects and in-mixing of old stratospheric air from the extratropics for the tape recorder. For this we will conduct additional sensitivity simulations without the effect of clouds/convection on $\delta\mathrm{D}(\mathrm{H_2O})$.
The individual influence of the two different monsoon systems, however, will still be addressed in the analysis and the revised discussion.
Due to the interhemispheric differences of lofted ice and its influence on $\delta\mathrm{D}(\mathrm{H_2O})$ in stratospheric water vapour, the ice lofting analysis (Sect. 6) will be used as motivation at the beginning of the section.

- *2) Method description:*

  Although this is a follow-up paper of a Part 1, I think it would be helpful for the reader to briefly summarize the main processes affecting HDO and their representation in the model (e.g., in section 2).

  2. We will include a couple of summarizing sentences with reference to Part 1 in the introduction.

- *P29464, L20: Can you discuss possible reasons for the dry bias of EMAC water vapor?*

  3. This is a well known issue in many models. The main reasons for this are a too cold tropopause and possibly a too coarse model grid. We will include this in the manuscript.

- *P29469, L14: This air originates from the westerly wind regime at around 40N over the Asian continent, because a high potential vorticity gradient (not shown) north of this region prevents meridional air mass exchange (see e.g. Plumb, 2002).*

  Horizontal PV-gradients above the North-Western Pacific around 130E are much weaker and transport (in-mixing) feasible. (This is related to my major comment.) P294

  4. Thank you very much for this comment. We will change the manuscript accordingly and show a much deeper analysis of this effect. Please see point 1.5 for details.

- *P29470, L23ff: The patch with negative values between 30 and 50N and 15 and 17 km suggests that the lack of the southward wind component in the American region leaves more isotopically enriched water vapour at the higher altitudes of the American extratropics. I would think this region of negative anomaly in Fig. 9 simply reflects the low δD within the ASM core (compare to Fig. 7).*

  5. Thank you, you are probably right. However, due to the methodological issue (reply to referee #1 point 11) and the discussion above, we will remove this figure.

- *For that, the anomalies w.r.t. the 21 year average of the δD(H2O) values between the 370 and the 390 K isentropes in the subtropical Western Pacific (15 to 40N and 120E to 140W) region and in the subtropical American and Western Atlantic region (15 to 40N and 120 to 20W)...*

  The defined ASM region includes not the monsoon core, only the downstream region (where in-mixing occurs), while the defined NAM region includes both (NAM core and related in-mixing). This seems to be not a proper comparison of related effects. Consequently, the interpretation in P29472/L4ff that This correlation analysis confirms the connection between the strength of the Monsoon systems... mixes the different effects of convective upward transport in the monsoons and in-mixing around the anticyclones.

  6. Thank you, among other reasons this comment leads us to remove the entire subsection and change the focus of this part of the manuscript (please see point 1.5).

- *P29476, L10ff: However, Randel et al. (2012) present a different behaviour of δD(H2O) in the UTLS by analysing ACE-FTS satellite data. In this retrieval, enriched δD(H2O) at 16.5 km altitude can be found only over America and the patch of high δD(H2O) associated with the ASM, as seen in the EMAC data is entirely lacking.*

  This is not true! Figure 10c in Randel et al. (2012) shows this patch as well (around 100E/15N), however weaker than in EMAC (and note that the ACE-FTS sampling density in this region is very low).

  7. Thank you for indicating that, we will change this sentence accordingly.

TECHNICAL CORRECTIONS

- P29460, L13: *...have a damping...*

  1. Thanks, will be corrected.

- P29461, L5: *...leads...*

  2. Thanks, will be corrected.

- P29461, L24: *...Eichinger et al. (2014)...*

  3. Thanks, will be corrected.

- P29462, L5: *A minus one is missing in the definition of δD*

  4. Absolutely, thank you very much for reading carefully.

- P29465, L5: *...processes are dominating...*

  5. Thanks, sounds better indeed.

- P29476, L5: *Later on,...*

  6. Thanks, will be corrected.

- Figs. 3/4: *...could be merged into a single figure.*

  7. Thanks, good idea.